Article

Revisiting Reduction of CO₂ to Oxalate with First-Row Transition Metals: Irreproducibility, Ambiguous Analysis, and Conflicting Reactivity

Maximilian Marx, Holm Frauendorf, Anke Spannenberg, Helfried Neumann, and Matthias Beller*

Cite This: JACS Au 2022, 2, 731−744

Read Online

ACCESS | Metrics & More | Article Recommendations | SI Supporting Information

ABSTRACT: Construction of higher $C_{\geq 2}$ compounds from CO_2 constitutes an attractive transformation inspired by nature's strategy to build carbohydrates. However, controlled C−C bond formation from carbon dioxide using environmentally benign reductants remains a major challenge. In this respect, reductive dimerization of CO_2 to oxalate represents an important model reaction enabling investigations on the mechanism of this simplest CO_2 coupling reaction. Herein, we present common pitfalls encountered in CO_2 reduction, especially its reductive coupling, based on established protocols for the conversion of CO_2 into oxalate. Moreover, we provide an example to systematically assess these reactions. Based on our work, we highlight the importance of utilizing suitable orthogonal analytical methods and raise awareness of oxidative reactions that can

likewise result in the formation of oxalate without incorporation of CO_2. These results allow for the determination of key parameters, which can be used for tailoring of prospective catalytic systems and will promote the advancement of the entire field.

KEYWORDS: CO₂ reduction, CO₂ reductive coupling, oxalic acid, oxidation, Cu catalysis, Fe catalysis
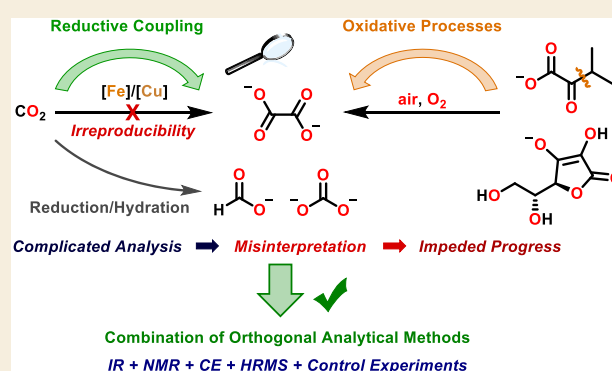
INTRODUCTION

Nature's ability to convert carbon dioxide (CO_2) into higher carbon compounds, mainly via photosynthesis, has inspired researchers for decades to evaluate the feasibility of constructing value-added $C_{\geq 2}$ materials from CO_2 as the starting material.[1,2] Various catalytic approaches enabling carbonylation,[3,4] carboxylation,[5−8] or copolymerization reactions[9,10] were developed based on CO_2 as a C_1 building block (Figure 1).[11] Moreover, the direct conversion into $C_{\geq 2}$ compounds, such as ethane,[12,13] ethylene,[14] ethanol and higher alcohols,[15−17] hydrocarbons,[18−20] and even aromatic compounds[21] has been achieved. Nonetheless, the selective formation of a $C_{\geq 2}$ product utilizing CO_2 under mild reaction conditions remains a significant challenge. This lack of development contrasts the significant progress for the CO_2 reduction to C_1 products, namely, methanol, carbon monoxide, formic acid, and methane via thermal, electrochemical, and photochemical approaches.[22−27] One of the major difficulties in the development of selective processes toward $C_{\geq 2}$ products resides in the C−C bond forming step.[18,19,21] Prior reduction of CO_2 to CO or methanol (MeOH) and subsequent conversion thereof to the final $C_{\geq 2}$ products circumvents this step.[16−19] However, a comprehensive understanding of the C−C bond formation starting from CO_2 might facilitate the development of tailored catalytic systems which could enable more selective transformations.
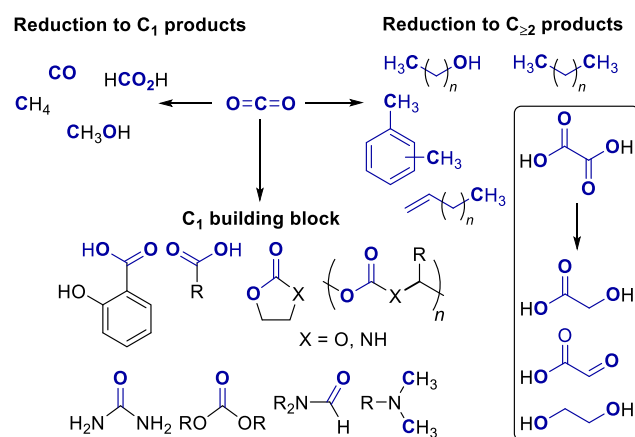
Figure 1. Selected examples highlighting the progress in CO_2 utilization as a C_1 building block or reduction into C_1 and $C_{\geq 2}$ products as well as potential products derived from oxalic acid.

Dimerization of two CO_2 molecules upon two-electron reduction resulting in oxalate, coined CO_2 reductive coupling, provides an ideal model reaction to investigate the C−C bond formation of interest. In addition, oxalic acid was recently suggested as a platform chemical for the preparation of sustainable polymers and its conversion into reduced C_2 compounds, such as glycolic acid and ethylene glycol.[28,29] Moreover, it is frequently applied in the purification and recycling of actinides by the nuclear industry.[30]

Early reports highlighted the formation of oxalate during electrochemical CO_2 reduction on inert electrodes (Hg and Pb).[31−34] Moreover, aromatic esters or nitriles,[33] as well as transition metal complexes,[35−41] were reported to be efficient electrocatalysts for this transformation.[25]

Nearly 40 years ago, a well-defined oxalate complex was isolated by Fröhlich and Schreer from the reaction of a titanium alkyl complex with CO_2.[42] Since this pivotal discovery, various oxalate complexes based on Mg,[43] Ti,[42,44] Sc,[45] Sm,[46−49] Yb,[48,50,51] Lu,[52] U,[53−55] Th,[56] Ni,[57,58] Fe,[59,60] and Cu (e.g., **2** and **3**)[39,61,62] were obtained from reaction with CO_2 (Figure 2).

Moreover, CO_2 reductive coupling with the help of strong chemical reductants, such as KC_8, was reported for complexes based on U,[55] Yb,[50] Fe (**1** and **5**),[63,64] Ni (**4**),[58] and Cu (**6a,b**).[65] Although all these studies were of limited practical relevance, they allowed for the identification of intriguing reaction pathways, e.g., dimetalloxycarbenes undergoing nucleophilic attack onto CO_2.[44,48,56] In addition, their homogeneous nature facilitated evaluation of the impact of steric and electronic parameters of the corresponding catalytic system onto oxalate formation.[47,48,60,65] However, the influence of reaction parameters, such as employed solvents or ligand properties, displayed major variations between different examples.

Likewise, the reaction mechanism for C−C bond formation appears to be rather specific for a respective system. Moreover, analysis of oxalate in the presence of additional CO_2 reduction products via NMR or IR spectroscopy can be challenging[66] and common analytic techniques for oxalate quantification[67−70] have scarcely been adopted within this field. These obstacles hamper systematic development of novel and refinement of existing protocols for the coupling of CO_2. Hence, the small number of reports on CO_2 reductive coupling compared to well-established CO_2 reduction to CO, formic acid, and $MeOH$[22−25] comes as no surprise. Further complication arises from undesired side reactions and irreproducibility of experimental results.[66,71,72] As an example, in situ analysis by Knope et al. on the formation of a Nd-based oxalate coordination polymer suggested that oxalate formation under hydrothermal conditions arose from oxidative decomposition of 2,3-pyrazinedicarboxylic acid without previously suggested incorporation of CO_2.[72] Similarly, in a joint cooperation with Maverick and co-workers, the oxidative decomposition of ascorbate, utilized as reductant for the formation of a Cu^I species, was identified as the source of the observed oxalate.[66] In this case, isolation of a dinuclear Cu oxalate complex in combination with a misleading difference IR spectrum and air contamination of reactions under CO_2 atmosphere caused misinterpretation of the experimental data. Such conflicting reactions provide the basis for incorrect interpretation of data and exacerbate the unsteady progress within this field.

Here, we present a guideline for investigations on the simplest C−C bond formation from CO_2 and showcase common pitfalls associated with this reaction. For this, three exemplary protocols based on first-row transition metals that have been reported to facilitate the reductive coupling of CO_2 were revisited in detail.

As a first example, the reaction of carbon dioxide and $[Fe(tmtaa)]$ (**1**, tmtaa = 4,11-dihydro-5,7,12,14-tetramethyldibenzo$[b,i]$-[1,4,8,11]-tetraazacyclotetradecine) in combination with strong reductants (Na, K, $NaC_{10}H_8$) is reexamined (Figure 2).[63] $[Fe^I(tmtaa)Na(THF)_3]$ (**7**), obtained by reduction of $[Fe^{II}(tmtaa)]$ with Na (−3.04 V vs Fc/Fc$^+$)[73] in THF, was reported to show a decisive solvent effect for its reaction with CO_2.[63] Reductive disproportionation of CO_2 to $[Fe^{II}(tmtaa)(CO)(THF)]$ (**8**) and Na_2CO_3 was described for the reaction in THF, while in toluene, the formation of oxalate (alongside **1**) was claimed based on titration with $KMnO_4$.

The coupling of CO_2 to oxalate in the absence of strong chemical reductants is evaluated on the example of a triazacyclononane-derived Cu^I complex. The allylated tridentate ligand **L1** was reported to facilitate the formation of dinuclear complex $[(L1)Cu(\mu\text{-}C_2O_4)Cu(L1)](BPh_4)_2$ (**2**) upon reaction of the in situ formed $[Cu(L1)]BPh_4$ complex with exhaled air, CO_2 (21%), and $CsHCO_3$ (53%) (Figure 2).[61]

Finally, the incorporation of CO_2 into oxalate starting from a Cu^{II} α-ketocarboxylate complex $[Cu(Tp^{iPr,iPr})(O_2CC(O)CH(CH_3)_2)]$ (**9**) under oxidative conditions with air, O_2, or CO_2/O_2 via a proposed $CO_2^{\bullet-}$ is reviewed.[62] Incorporation of CO_2 into the product **3** (Figure 2) was reported based on a reaction with $^{13}CO_2/O_2$ and vibrational spectroscopy.

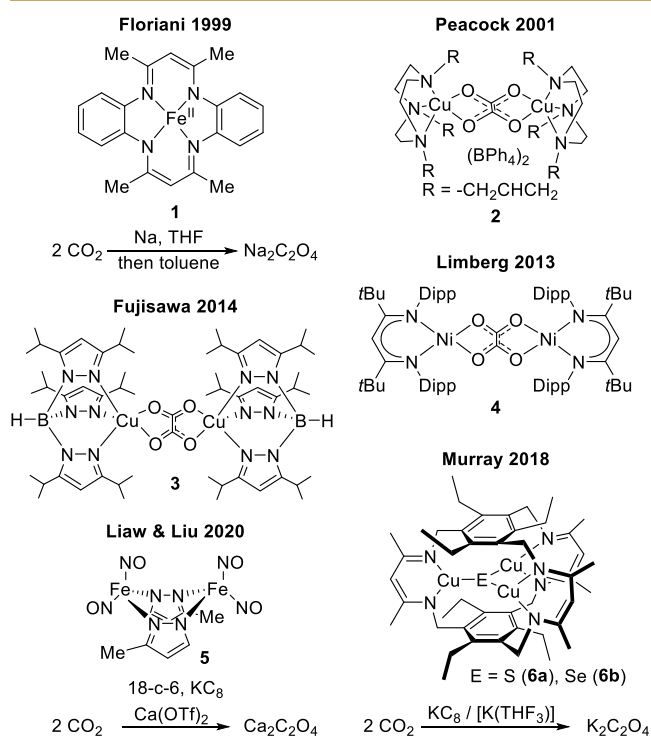In all these cases, incorporation of CO_2 into oxalate proved to be irreproducible.

Figure 2. Selected examples for the formation of oxalate complexes from CO_2 and CO_2 reductive coupling with strong reductants.[58,61−65] The reactions with complexes **1**−**3** are discussed herein.

RESULTS

Reactions with [Fe(tmtaa)]

Based on the previous work, we initiated our investigations by studying the reaction of in situ formed **7** with CO_2 in toluene

Scheme 1. Reduction of [Fe(tmtaa)] to Complex 7 and Observed Products of Subsequent Reaction with CO_2 Highlighting the Absence of Oxalate
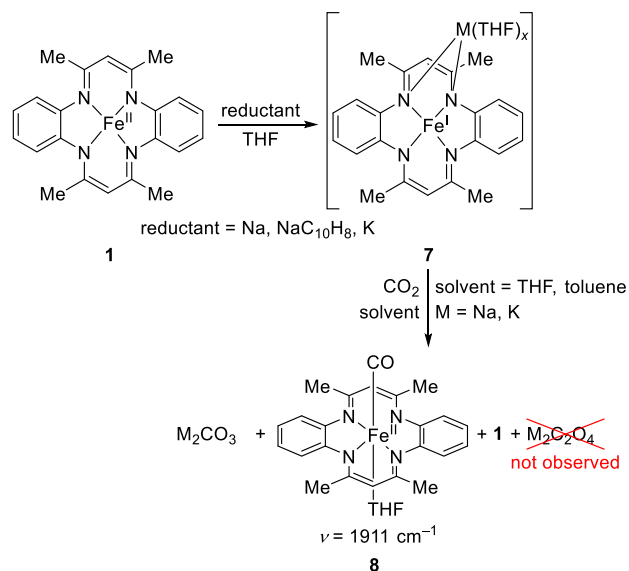
(Scheme 1). In our hands, we were unable to identify oxalate by ^{13}C NMR spectroscopy (Figures S52 and S53) and capillary electrophoresis (<0.5% yield based on [Fe]; Figures S349 and S350) after aqueous extraction of the reaction mixture, despite the utilization of excess sodium (Table S1, detailed procedures and results are presented in the Supporting Information). To rule out the insufficient solubility of Na causing the lack of $C_2O_4^{2-}$ formation, further reactions were conducted utilizing $NaC_{10}H_8$ (-3.10 V vs Fc/Fc$^+$)[73] in THF as the reductant for in situ formation of **7**. Again, no $C_2O_4^{2-}$ was observed by NMR spectroscopic (Figures S50 and S51) and CE analysis (Figures S347 and S348). To complement the data obtained with Na-based reductants, analogous reactions were performed with K.

In these cases, reaction in THF and toluene also provided no evidence for the reductive coupling of CO_2. However, a signal in the ^{13}C NMR spectra located between 162 and 164 ppm was observed for all reactions (Figures S50–S59), which was assigned to CO_3^{2-} by adjustment of the pH value of the NMR sample (with 1 M NaOH) and comparison with Na_2CO_3 (Figure S49). The formation of carbonate in both THF and toluene suggests an accompanied CO_2 reduction to CO regardless of the solvent. This was indeed confirmed by the presence of the distinct CO vibration[63] (1911–1912 cm^{-1}) of iron carbonyl complex **8** in the IR spectra of the solid product from the reaction of **1** with K in THF and subsequent treatment with CO_2 in THF or toluene (Figures S190–S196). Interestingly, no gaseous CO was found during gas chromatographic analysis of the reaction headspace (Figure S456). NMR analysis of the residue after treatment with K and CO_2 revealed the presence of **1**[63] for the reaction in toluene, while line broadening, presumably due to paramagnetism, prohibited assignment to **1** or **8** for the reaction in THF (Figure S48).

Based on these results, we found no evidence for the formation of oxalate utilizing complex **1** and strong chemical reductants while reductive disproportionation was confirmed in both THF and toluene.

CO_2 Reductive Coupling by tacn-Derived Cu Complexes [Cu(L)]X

We initiated our investigations on the oxalate formation with **L1** reported by Peacock and co-workers by following the literature protocols.[61] In our hands, CO_2 bubbling through a suspension of CuI, **L1**, and NaBPh$_4$ in MeOH resulted in a color change, indicating oxidation of the Cu^I complex. However, the residue obtained from this experiment featured an IR band at 1628 cm^{-1} (Figure S197), significantly shifted compared to the literature value of 1660 cm^{-1},[61] and recrystallization from MeNO$_2$ did not provide the desired oxalate complex. Interestingly, when CO_2 bubbling was paused after an initial saturation of the reaction mixture over 2 h and the mixture was stirred overnight under an Ar/CO_2 atmosphere, a decolorization was observed that was repeatable for the same reaction mixture (up to six times, see Figure S1). This color change indicated a reversible oxidation of the Cu^I complex during CO_2 bubbling, possibly accompanied by reduction of a Cu^{II} complex by NaBPh$_4$.[74] Reaction with NaPF$_6$ instead of NaBPh$_4$ did not cause a decolorization upon paused CO_2 bubbling, thus corroborating the role of BPh$_4^-$ in the reduction. The color change during reactions with CO_2 in the presence of NaBPh$_4$ was accompanied by precipitation of a yellow solid. NMR spectroscopic analysis of this precipitate (in THF-d_8) indicated the formation of a Cu^I complex different from [Cu(**L1**)I][75] (Figure S61), presumably [Cu(**L1**)]BPh$_4$ based on the absence of additional signals in the ^{13}C NMR and the integral ratio in the ^1H NMR spectrum. Contact of the THF-d_8 solution to air resulted in crystallization of [(**L1**)Cu(μ-OH)$_2$Cu(**L1**)](BPh$_4$)$_2$ (**10**, Figure 3), which is in good
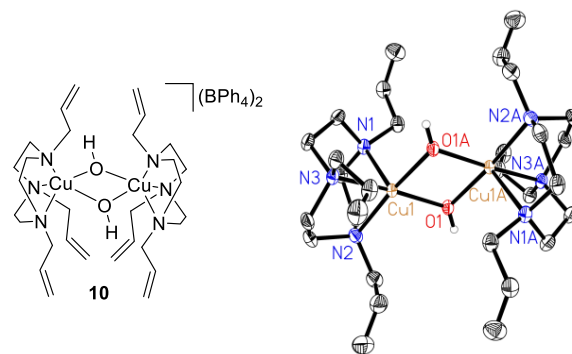
Figure 3. Compound **10** and the molecular structure of [(**L1**)Cu(μ-OH)$_2$Cu(**L1**)]$^{2+}$ in **10** (thermal ellipsoids displayed at 30% probability and C-bound H atoms omitted for clarity; symmetry operator for generating equivalent atoms: $-x + 1$, $-y + 1$, $-z + 1$).

accordance with analogous compounds formed via aerial oxidation of the Cu^I complexes.[76,77] However, the desired oxalate complex was not obtained from these experiments, and IR vibrations were observed around 1630 cm^{-1}, thus shifted by 30 cm^{-1}.

Inspired by the possibility of removing potentially formed oxalate from the product complex,[62] we attempted the synthesis of complex **2** starting from $Na_2C_2O_4$. While a reaction utilizing in situ formed [Cu(**L1**)(NO$_3$)$_2$] (**11**) provided a mononuclear complex [Cu(**L1**)(κ^2-C_2O_4)] (**12**), we were able to obtain blue needles of [(**L1**)Cu(μ-C_2O_4)Cu(**L1**)](BF$_4$)$_2$ (**13**) in 62% yield

utilizing $Cu(BF_4)_2 \cdot 6H_2O$ and $Na_2C_2O_4$ in $MeOH/H_2O$. As expected, the coordination geometry in **13** is similar to that of **2** (Figure 4). Moreover, its distinct C−O stretching vibration is observed at 1651 cm^{-1} (Figure S178).
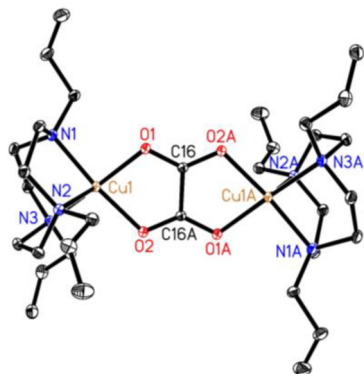

Figure 4. Molecular structure of $[(\mathbf{L1})Cu(\mu\text{-}C_2O_4)Cu(\mathbf{L1})]^{2+}$ in **13** (thermal ellipsoids displayed at 30% probability and H atoms omitted for clarity; symmetry operator for generating equivalent atoms: $-x, -y + 1, -z + 1$).

With $[(\mathbf{L1})Cu(\mu\text{-}C_2O_4)Cu(\mathbf{L1})](BF_4)_2$ in hand, we assessed the removal of $C_2O_4^{2-}$ by stirring in toluene/1 M NaOH (2:1, v:v).[62] To our delight, we detected $C_2O_4^{2-}$ with a yield of 47% by CE for two reactions on 24 μmol scale (**1**, 48%; **2**, 47%). On this scale, the ^{13}C NMR signal of $C_2O_4^{2-}$ at 173 ppm (Figure S60 provides ^{13}C NMR shifts for common CO_2 reduction products in D_2O) was not observable (however, a minor broadening of the baseline for reaction 1 was noticed).

Having established the possibility of oxalate removal from the desired dinuclear Cu complex, we turned our attention to the reaction with solid bicarbonates, which was supposed to yield higher quantities of complex **2**.[61] It is noteworthy that we isolated $[Cu(\mathbf{L1})Cl_2]$ (**14**) from an initial reaction of CuI/**L1**/NaBPh$_4$ (1:1:1) with CsHCO$_3$ (1.3 equiv) in MeOH following filtration, column chromatographic separation (SiO$_2$, MeOH/MeNO$_2$/2 M NH$_4$Cl, 7:1:2), and recrystallization from hot MeNO$_2$. **14**, which can be independently prepared from CuCl$_2$, presumably results from oxidation of the initial Cu^I complex during the aerial workup and subsequent ligand exchange with NH$_4$Cl during purification.

Additional reactions (Table 1) with CsHCO$_3$ or NaHCO$_3$ in combination with CuI or $[Cu(MeCN)_4]PF_6$ in MeOH did not result in notable oxalate formation (according to NMR and CE analysis). Notably, a broad signal coinciding with the oxalate signal was observed for the reactions with CuI in the absence of NaBPh$_4$ (Table 1, entries 5−6; Figures S368 and S369). However, no oxalate was detected by ESI-HRMS analysis for entry 6 (Figure S305), suggesting the presence of another compound with a similar migration time. In this case, most likely the iodide anion was detected as the mobility constants for oxalate and I$^-$ are comparable.[78] Indeed, control measurements confirm this behavior (Figure S357).

Due to the lack of oxalate formation by CO_2 bubbling and reaction with MHCO$_3$, we evaluated the exposure of in situ formed $[Cu(\mathbf{L1})]X$ (X = I, BPh$_4$) to air to rule out an oxidative origin of oxalate. However, leaving a suspension of CuI, **L1**, and NaBPh$_4$ in MeOH or MeOH/EtOH (1:4, v:v) in air over 41 and 1 d, respectively, did not result in substantial $C_2O_4^{2-}$ formation according to CE (Table S4).

Table 1. Treatment of In Situ Formed Cu-tacn Complexes with Bicarbonates[a]

entry	[Cu] [μmol]	[MHCO$_3$] [μmol]	t [h]	^{13}C NMR ($C_2O_4^{2-}$)	CE ($C_2O_4^{2-}$ (?)) [%][b]
1	CuI (126)	CsHCO$_3$ (133)	16	n.d.	<1
2	CuI (120)	CsHCO$_3$ (126)	117	n.d.	<1
3[c]	CuI (150)	CsHCO$_3$ (300)	168	n.d.	<0.5
4[d]	CuI (296)	NaHCO$_3$ (214)	210	n.d.	<1
5[e]	CuI (126)	CsHCO$_3$ (134)	17	n.d.	11
6[e]	CuI (122)	CsHCO$_3$ (129)	122	n.d.	7
7[f]	[Cu] (120)	CsHCO$_3$ (127)	118	n.d.	<0.5
8[f]	[Cu] (120)	NaHCO$_3$ (127)	118	n.d.	<1

[a]Reaction conditions: [Cu]/**L1**/NaBPh$_4$ (1:1:1) combinations were utilized in degassed MeOH. n.d. = not detected. [b]Oxalate yields were calculated for signals coinciding with Na$_2$C$_2$O$_4$ added as internal standard after initial measurement and were found to overlap with the signal of iodide. [c]NaPF$_6$ (1.2 equiv) instead of NaBPh$_4$ was utilized. [d]1.7 equiv of CuI was utilized. [e]Reaction in the absence of NaBPh$_4$. [f]Reaction with $[Cu(MeCN)_4]PF_6$.

Likewise, treatment of the in situ formed Cu^I complex with O_2 did not cause formation of oxalate. Interestingly, peaks likely belonging to I$^-$ with integrals corresponding to $C_2O_4^{2-}$ yields of 7% and 6% were observed for the exposure of solutions of in situ formed $[Cu(\mathbf{L1})I]$ to air in the absence of NaBPh$_4$ (Figures S375 and S376).

Due to the absence of oxalate formation in all these experiments, we investigated the impact of reaction parameters to possibly facilitate CO_2 reductive coupling (Table 2).

Prolonged stirring under a constant CO_2 atmosphere for 5 days (Table 2, entries 2 and 3) did not provide detectable quantities of oxalate. Likewise, changing the solvent to a mixture of MeOH and THF (Table 2, entry 4), THF (Table 2, entry 5), or toluene (Table 2, entry 6) as well as illuminating the reaction mixture with visible light (400−700 nm, 0.09 W; Table 2, entry 9) remained unsuccessful. Interestingly, elevated temperature (40 °C, entries 7 and 8) and elevated CO_2 pressure (10 bar, entries 10 and 11) facilitated the appearance of a signal of fitting migration time in the CE analysis (Figures S384−S386, S388, S389), corresponding to 5% and 14% $C_2O_4^{2-}$ yield, respectively (average of two reactions). Again, no oxalate was found by ESI-HRMS analysis, indicating yet again overlapping with the signal of iodide. However, ion suppression during the electrospray ionization process has to be considered and can be controlled by further dilution, adding an internal standard ion, or by coupling with CE.

Various additives, namely, $Mg(OTf)_2$, $LiBF_4$, HCO$_2$Na, and KPF_6, showed no improvement of the reactivity when combined with CuI or $[Cu(MeCN)_4]PF_6$ and ligand **L1** (Table S6). Since iodide exchange with NaBPh$_4$ was found to be incomplete,

Table 2. Treatment of CuI, NaBPh₄, and L1 with CO₂ under Varying Reactions Conditions[a]
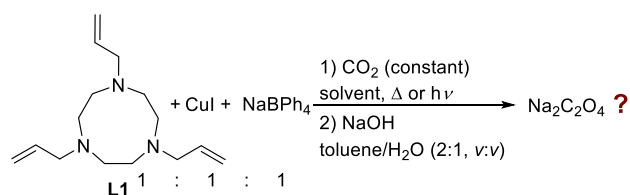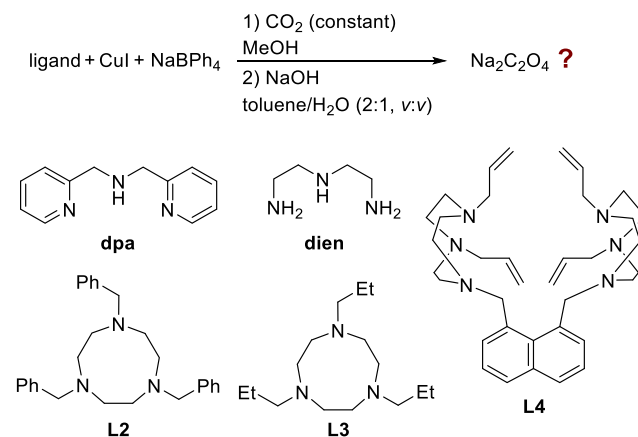

entry	CuI [μmol]	parameter	t [h]	^{13}C NMR ($C_2O_4^{2-}$)	CE ($C_2O_4^{2-}$ (?)) [%][b]
1	120	-	24	n.d.	<1
2	120	-	118	n.d.	<0.5
3	182	-	120	n.d.	<0.5
4	120	MeOH/THF (9:1)	118	n.d.	<0.5
5	124	THF	120	n.d.	<0.5
6	123	toluene	121	n.d.	<1
7	120	40 °C	114	n.d.	3
8	122	40 °C	123	n.d.	8
9	133	400−700 nm (0.09 W)	18	n.d.	<0.5
10	130	10 bar	116	n.d.	16
11	132	10 bar	116	n.d.	12

[a]Reaction conditions: CuI/**L1**/NaBPh₄ (1:1:1) was utilized in degassed MeOH under constant CO₂ atmosphere, unless indicated by the varied parameter. n.d. = not detected. [b]Oxalate yields were calculated for signals coinciding with Na₂C₂O₄ added as internal standard after initial measurement and were found to overlap with the signal of iodide.

indicated by the crystallization of [Cu(**L1**)I] (**15**) from a THF solution of CuI, NaBPh₄, and **L1**, dehalogenation with AgBPh₄ was conducted. However, no improvement of the reaction was detected by CE/NMR analysis after NaOH treatment (2% yield by CE, but integration hampered by partial overlapping; Figure S391), despite an IR signal at 1665 cm⁻¹ (Figure S235). Interestingly, oxalate in low yields was detected for reactions with NaC₁₀H₈ in THF, even in the absence of any Cu complex (2−7% yield).

Next, other tridentate N-based ligands were evaluated instead of **L1** (Table 3). Unfortunately, dipicolylamine (**dpa**), 1,4,7-benzylated (**L2**), and 1,4,7-propylated (**L3**) tacn showed no evidence for CO₂ reductive coupling reactivity. In contrast, diethylenetriamine (**dien**) clearly showcased the limits of CE analysis. A signal that would correspond to a 28% C₂O₄²⁻ yield was observed for a reaction of CO₂ with **dien**, CuI, and NaBPh₄ in MeOH over 5 d (Table 3, entry 4). No intense C−O vibration was observed above 1600 cm⁻¹ (Figures S255 and S256), and doubling the reaction scale caused a noticeable decrease in the potential C₂O₄²⁻ yield to 10% (Table 3, entry 5). Moreover, performing the reaction under an argon atmosphere resulted in the same CE signal (Figure S414), meaning that the CE signal is most likely corresponding to I⁻ rather than a CO₂ reduction product.

To evaluate if dinuclear Cu complexes might offer an intrinsic advantage for the reductive coupling of two CO₂ molecules, we envisaged ligand **L4** as a prime candidate. Thus, we targeted the allyl-derivative **L4** which was prepared by reaction of 1,4,7-triazatricyclo[5.2.1.0⁴,¹⁰]decane (**16**)[79] with 1,8-bis-(bromomethyl)naphthalene (**17**)[80] and subsequent allylation (Scheme 2). Isolation of [Cu₂(**L4**)I₂] (**19**) further showcased the ability of **L4** to coordinate to two Cu centers.

Table 3. Treatment of CuI, NaBPh₄, and Different Ligands with CO₂ in MeOH[a]

entry	CuI [μmol]	ligand	t [h]	^{13}C NMR ($C_2O_4^{2-}$)	CE ($C_2O_4^{2-}$ (?)) [%][b]
1	123	**L2**	120	n.d.	<0.5
2	124	**L3**	120	n.d.	<0.5
3	151	**dpa**	120	n.d.	2
4	184	**dien**	119	n.d.	28
5	409	**dien**	119	n.d.	10
6[c]	180	**dien**	120	n.d.	26
7	53	**L4**	114	n.d.	5
8[d]	63	**L4**	118	n.d.	29
9[d]	187	**L4**	119	n.d.	19
10[d,e]	187	**L4**	119	n.d.	28
11[d,f]	94	**L4**	118	n.d.	32
12[c,d]	63	**L4**	124	n.d.	3
13[c,d]	94	**L4**	118	n.d.	<0.5

[a]Reaction conditions: CuI/**ligand**/NaBPh₄ (1:1:1) was utilized in degassed MeOH under constant CO₂ atmosphere, unless stated otherwise. n.d. = not detected. [b]Oxalate yields were calculated for signals coinciding with Na₂C₂O₄ added as internal standard after initial measurement and were found to overlap with the signal of iodide. [c]Reaction conducted under Ar. [d]A total of 0.5 equiv of **L4** was utilized. [e]Reaction conducted with ¹³CO₂. [f]Reaction conducted without NaBPh₄.

Scheme 2. Synthesis of Ligand L4 and Its Derived Cu^I Complex 19 and (Left) Molecular Structure of 19[a]
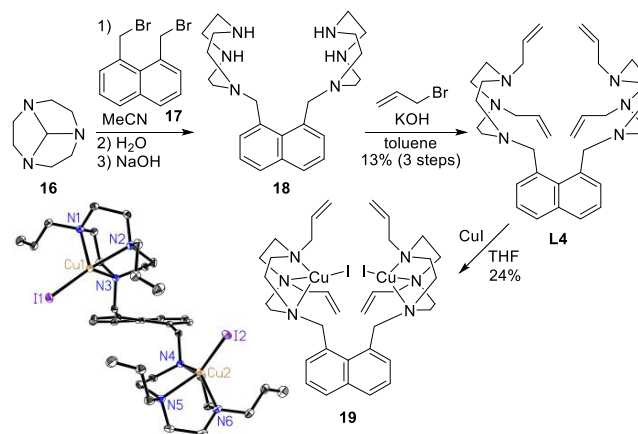
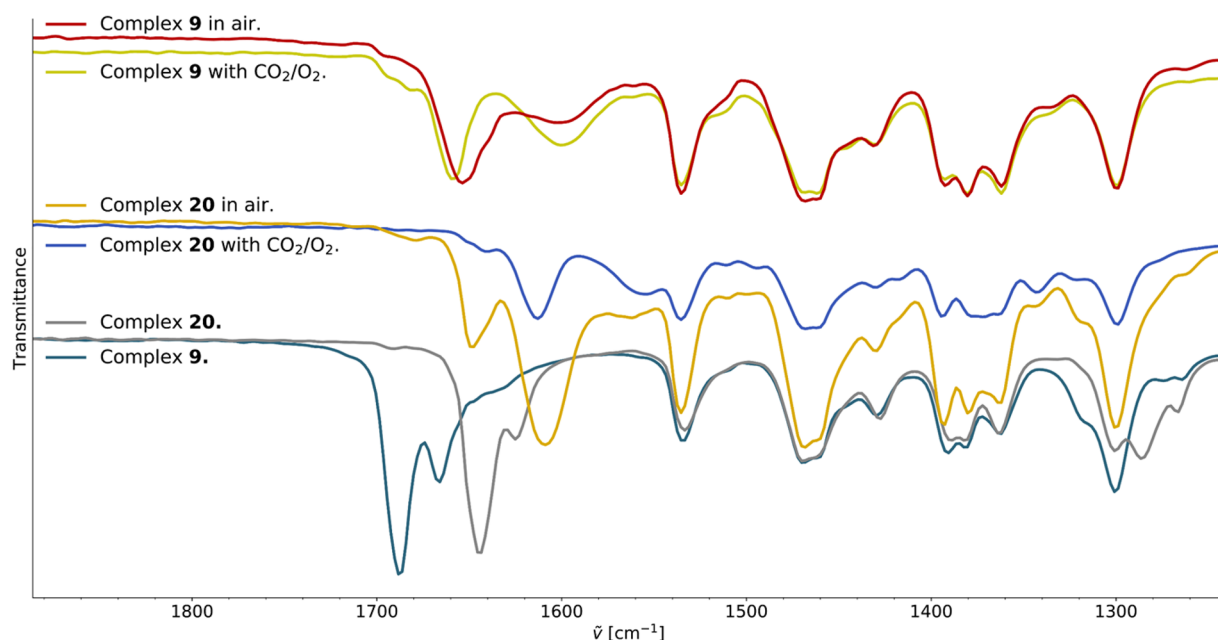[a]Thermal ellipsoids are displayed at 30% probability, and H atoms are omitted for clarity.

Figure 5. FTIR spectra from reaction of complexes **9** and **20** with air and CO_2/O_2 in DCM and toluene, respectively (FTIR spectra of **9** and **20** are displayed for comparison).

Reactions of **L4**, CuI, and $NaBPh_4$ toward CO_2 in MeOH resulted in the appearance of a CE signal corresponding to 29% $C_2O_4^{2-}$ yield (Table 3, entry 8; 32% in the absence of $NaBPh_4$, entry 11) which decreased to 19% upon increase of the reaction scale (Table 3, entry 9). Contrary to previous experiments with **dien**, blank experiments under argon did not result in the appearance of this CE peak (≤3% yield; Table 3, entries 12 and 13; Figures S421 and S422). However, no oxalate was detected by ESI-HRMS analysis (Figure S312). Moreover, an experiment with $^{13}CO_2$ (formed from $Na_2^{13}CO_3$ and H_2SO_4), yielding a signal suggesting a 28% $C_2O_4^{2-}$ yield by CE, displayed no observable oxalate signal in the ^{13}C NMR spectrum (Figure S127).

Hence, we exclude the formation of substantial quantities of oxalate with novel ligand **L4** as well as **L1**, **L2**, **L3**, **dien**, and **dpa** under the studied reaction conditions.

Reactions of α-Ketocarboxylates and Derived CuTp Complexes toward CO_2

To evaluate the third literature example, we prepared complex **9** and its $^{13}C_5$-labeled congener **20** (84%) following the same procedure[62] but utilizing sodium $^{13}C_5$-3-methyl-2-oxobutyrate (**21**). ^{13}C-labeling resulted in the expected shift of the C−O stretching frequencies from 1666/1687 cm^{-1} (**9**) to 1625/1644 cm^{-1} (**20**) (Figure 5).

Exposure of **9** and **20** to air (Scheme 3) caused an alteration of the IR spectra resulting in new bands at 1655 cm^{-1} and a broad band at 1602 cm^{-1} for **9**, the former being in accordance with the initial report.[62] For **20**, signals at 1609 and 1644 cm^{-1} were observed in addition to a broadened band at 1562 cm^{-1} (Figure 5). The former is in agreement with the isotopic shift observed by Takisawa et al. while the latter two remained inconclusive.

Therefore, the obtained products were extracted with NaOH and analyzed by NMR spectroscopy and CE. Indeed, the formation of oxalate could be verified (Figures S133−S134 and S423−S425); however, the observed yields (**9**: 7% [18 h], 54% [48 h]; **20**: 23% [18 h]) were significantly decreased in comparison to the literature (89%).[62] It is noteworthy that these

Scheme 3. Reaction of Complexes 9 or 20 with Air or CO_2/O_2 and Subsequent Treatment with NaOH in H_2O/Toluene
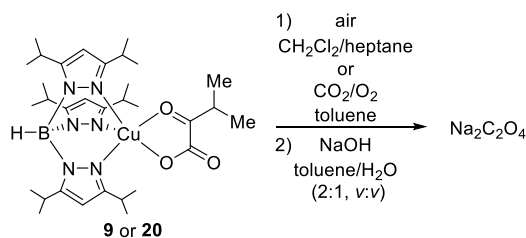
yields are determined by CE and calculated assuming a bimolecular mechanism with one oxalate being formed from two α-ketocarboxylate complexes. ^{13}C NMR spectroscopy for the reaction of **20** allowed for the identification of two major byproducts, namely, 2-hydroxy-2-methylpropanoic acid (confirmed by ESI-HRMS; Figure S317) and 2-methylpropanoic acid (Figure 6).

When reactions of **9** and **20** were conducted in toluene under an O_2/CO_2 atmosphere, analogous IR spectra were obtained (Figure 5). Again, $C_2O_4^{2-}$ yields quantified by CE were significantly reduced (**9**: 7%; **20**: 2%), and 2-hydroxy-2-methylpropanoic acid as well as 2-methylpropanoic acid were detected as the primary products by ^{13}C NMR spectroscopy after NaOH extraction (Figure S149−S151). Interestingly, addition of minor quantities of D_2O to the reaction of **20** with CO_2/O_2 in toluene-d_8 and analysis by ^{13}C NMR spectroscopy revealed the formation of $^{13}C_3$-acetone (203.7 ppm [t], 30.3 ppm [d], Figure S131). Subsequent extraction with NaOH and analysis by NMR spectroscopy suggested higher selectivities for $C_2O_4^{2-}$ formation (compare Figure S151 and Figures S153 and S155), while yields assessed by CE were poorly reproducible (25% and 3% for two reactions). Nonetheless, the higher selectivity for $C_2O_4^{2-}$ in the presence of D_2O appears to be in accordance with the literature.[62] In addition, ESI-HRMS analysis for reactions of **20** in air and under CO_2/O_2 atmosphere showed no evidence for the presence of $^{13}C^{12}CO_4^{2-}$, while
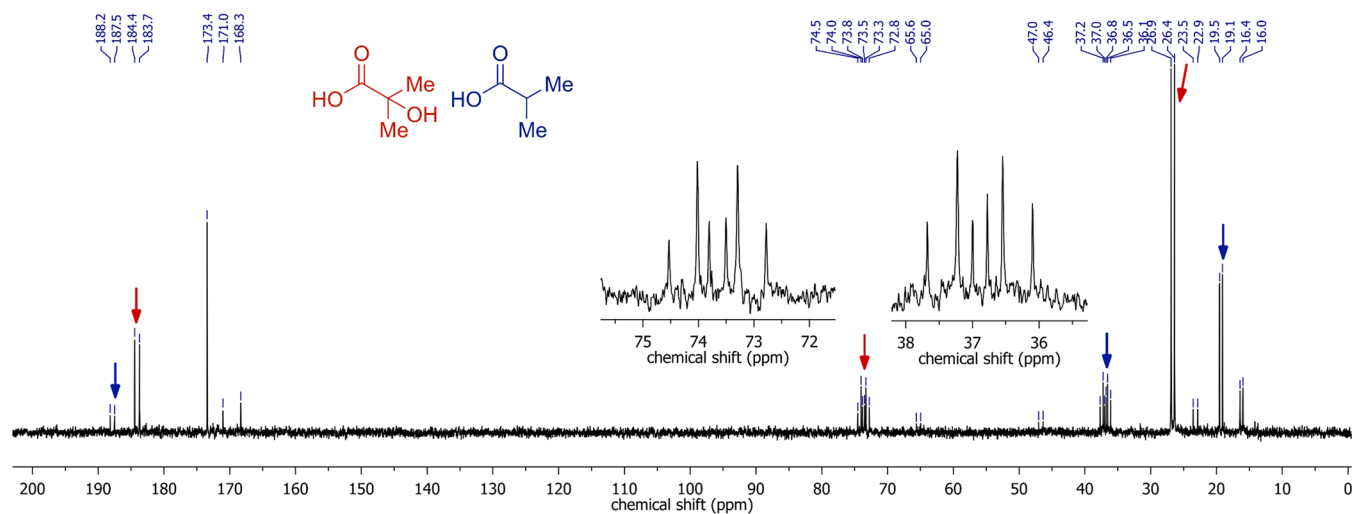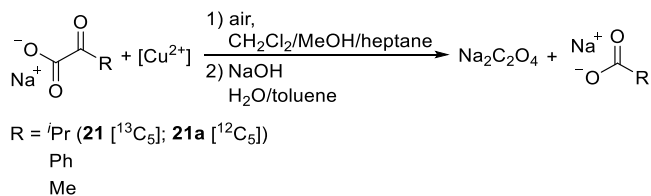
Figure 6. ^{13}C NMR spectroscopic analysis of the NaOH extract from the reaction of **20** with air.

^{13}C$_2$O$_4$$^{2-}$ was detected for the former and the reaction with CO$_2$/O$_2$ in toluene-d_8/D$_2$O (Section S9.2).

Next, in situ formation of **20** starting from CuCl$_2$, sodium ^{13}C$_5$-3-methyl-2-oxobutyrate (**21**), and KTp^{iPr,iPr} in DCM/heptane and exposure to air was attempted and resulted in an oxalate yield of 38% (CE) after 27 h.

To gain further insight into the oxalate formation and evaluate the necessity of defined complexes **9**/**20**, analogous reactions were conducted in the absence of the Tp^{iPr,iPr} ligand (Scheme 4).

Scheme 4. Reactions of Different Sodium α-Ketocarboxylates in Combination with a Cu^{2+} Source under Oxidative Conditions and Subsequent NaOH Treatment for Analysis via NMR and CE

R = ^{i}Pr (**21** [^{13}C$_5$]; **21a** [^{12}C$_5$])
    Ph
    Me

For this purpose, a Cu precursor and sodium 3-methyl-2-oxobutyrate (**21a**) were suspended in DCM containing 10% MeOH and left in air (layered with heptane). Subsequent NaOH treatment revealed the formation of oxalate as the major product with 1 equiv of Cu(BF$_4$)$_2$·6H$_2$O (38−59% by CE, Table S8) or CuCl$_2$ (55−82%). Note that oxalate yields from here on are monomolecular yields assuming one C$_2$O$_4$$^{2-}$ per α-ketocarboxylate. In addition, substoichiometric quantities of Cu(BF$_4$)$_2$·6H$_2$O (0.2 equiv) were sufficient to provide 48% C$_2$O$_4$$^{2-}$. In the absence of Cu, 4% C$_2$O$_4$$^{2-}$ was detected by CE (Figure S446), while only the starting material was observed by IR spectroscopy (Figure S292).

In addition to these aerial oxidations, Cu(BF$_4$)$_2$·6H$_2$O and **21** were stirred under a CO$_2$/O$_2$ atmosphere in CD$_2$Cl$_2$/CD$_3$OD (10:1, v:v) and C$_6$D$_6$/CD$_3$OD (10:1, v:v) for 4 d. In these cases, ^{13}C NMR spectroscopic analysis confirmed the formation of ^{13}C$_3$-acetone (Figure S131). Subsequent NaOH treatment provided oxalate in 19% (CD$_2$Cl$_2$) and 39% (C$_6$D$_6$) yield, respectively. The former was lower due to a noticeable amount of 2-methylpropionic acid resulting from decarboxylation

(Figures S156 and S158). The reason for the favored decarboxylation in CD$_2$Cl$_2$ is not clear and might be a result of DCl traces. It should be noted that in no case mixed isotopic constitutions of C$_2$O$_4$$^{2-}$ were detected by ESI-HRMS analysis (Section S9.2), substantiating the lack of CO$_2$ incorporation starting from both, defined complexes **9**/**20**, or a Cu^{II} salt combined with the α-ketocarboxylate.

Interestingly, NaOH treatment under an Ar atmosphere decreased the oxalate yield to 17% (from 49% in air, Tables S8 and S10), and significant quantities of starting material were observed by ^{13}C NMR spectroscopy (Figures S163 and S164).

Finally, evaluation of different α-ketocarboxylates was performed to complement the results of our investigation. The reaction of sodium phenylpyruvate with Cu(BF$_4$)$_2$·6H$_2$O in DCM/MeOH in air over 46 h resulted in 29% oxalate (CE). In contrast, sodium pyruvate gave only 6% by CE after 16 h, close to the blank experiment. However, we observed oxidative decarboxylation to acetate by ^{13}C NMR spectroscopy (Figure S165). Moreover, 2-hydroxy-3-methylbutyric acid did not undergo oxidative degradation to oxalate.

While the formation of oxalate was confirmed for defined complexes **9** and **20** as well as for reactions in the absence of Tp^{iPr,iPr}, we found no evidence for the incorporation of CO$_2$ into the product oxalate and, thus, cannot confirm the reported conversion of CO$_2$ into oxalate.

■ DISCUSSION

Reduction of [Fe^{II}(tmtaa)] with Na in THF, yielding [Fe^I(tmtaa)Na(THF)$_3$] (**7**), and subsequent reaction with CO$_2$ was reported to result in two distinct reactions depending on the employed solvent.[63] Formation of [Fe^{II}(tmtaa)(CO)-(THF)] (**8**) and Na$_2$CO$_3$ via reductive disproportionation of CO$_2$ was observed in THF. In contrast, oxalate was the claimed product from the reaction in toluene assessed by titration with KMnO$_4$.

Based on the previous work, we investigated the reaction starting from **1** and Na, NaC$_{10}$H$_8$, and K followed by treatment with CO$_2$ in toluene or THF (Scheme 5). For the reactions with K, we were able to confirm the formation of CO, in the form of complex **8**, and CO$_3$$^{3-}$ resulting from reductive disproportionation of CO$_2$. Yet, we did not observe the reported solvent effect and identified the distinct CO band of complex **8** (1911−1912 cm^{-1}) for reactions in both toluene and THF. Interestingly, we

Scheme 5. Revised Reaction of [Fe(tmtaa)] with Strong Reductants Followed by CO_2 Treatment Yielding "CO" and M_2CO_3 but Not $M_2C_2O_4$
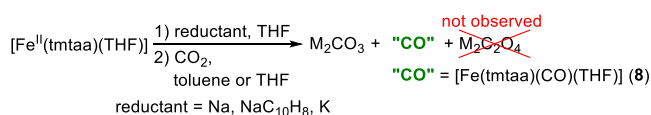
did not detect any oxalate by NMR spectroscopy or CE analysis (<0.5% based on **1**) after aqueous extraction of the resulting reaction products regardless of the utilized reductant, thus ruling out insufficient solubility preventing CO_2 reductive coupling.

This lack of oxalate formation highlights two major hurdles associated with studying the reduction of CO_2 into oxalate, namely, *irreproducibility* and *ambiguous analysis*. Standardization of $KMnO_4$ with the help of oxalate constitutes an established procedure.[81] However, $KMnO_4$ is likewise able to oxidize the metal catalyst (in this case Fe^{2+}) and most organic compounds.[82,83] Therefore, oxidation of residual Fe^{2+} or an organic impurity could have resulted in a false positive for the $KMnO_4$ titration. Thus, our results emphasized the importance of combining different analytical methods to confirm the presence of $C_2O_4^{2-}$. Furthermore, the reactions with [Fe(tmtaa)] showcased that strong reductants capable of facilitating $CO_2^{•-}$ formation do not guarantee reductive coupling to oxalate.

Our investigations on the second selected literature example further corroborate that both of these pitfalls are not limited to the single example of [Fe(tmtaa)]. Peacock and co-workers reported a Cu^I complex bearing an allylated tridentate ligand (**L1**) that was converted into the dinuclear complex [(**L1**)Cu(μ-C_2O_4)Cu(**L1**)](BPh_4)_2 (**2**) upon reaction with exhaled air, CO_2 (21%), or $CsHCO_3$ (53%) in MeOH.[61] Besides a characteristic IR signal at 1660 cm^{-1}, a crystal structure of the oxalate complex and its magnetic moment were reported to prove the reductive coupling of carbon dioxide. A major advantage of this approach seems to be the absence of additional reductant. Surprisingly, despite the interest in the chemistry of tacn-derived Cu complexes,[80,84−91] no further developments of this system were reported, possibly highlighting the unique properties of allyl-substituted **L1**.

In our hands, initial experiments with CO_2 bubbling indicated an oxidation of the Cu^I complex formed from CuI, $NaBPh_4$, and **L1**. However, isolation of a μ-hydroxo Cu^{II} complex (**10**) highlighted that trace O_2 might compromise the distinct color change associated with Cu^I oxidation as an analytical tool. Moreover, IR bands in the 1630 cm^{-1} region observed for the products from these CO_2 bubbling experiments might indicate the formation of a CO_2 reduction product, despite the 30 cm^{-1} difference with respect to desired complex **2**. Given the proximity of C−O vibrations of CO_2 derived compounds, such as $NaHCO_3$ or HCO_2Na in the 1550−1700 cm^{-1} range (Figure S197), additional analytical data for the identification of CO_2 reduction products was desirable. Therefore, we prepared the BF_4^- analogue of complex **2** and confirmed the possibility of oxalate removal by extraction with aqueous NaOH. This extraction after initial FTIR analysis allowed for detection of oxalate by CE and ^{13}C NMR as well as quantification by CE. With this methodology in hand, the conversion of solid bicarbonates into oxalate with a Cu^I source and **L1** was evaluated but provided no evidence for the reaction of interest. Likewise, evaluation of various reaction parameters, such as

solvents, temperature, CO_2 pressure, light, or different additives did not yield competing quantities of oxalate. As part of these experiments, a shortcoming of the CE analysis was encountered. Due to similar mobility constants of iodide and oxalate,[78] overlapping of their signals during CE analysis could be expected and was confirmed by control measurements. Moreover, we observed signals coinciding with oxalate especially for reactions in the absence of $NaBPh_4$ or at elevated temperature or pressure. Nonetheless, ESI-HRMS showed no evidence for oxalate formation, substantiating that these signals result from I^- rather than $C_2O_4^{2-}$.

Thus, for a precise determination of oxalate in such and related processes, the use of different analytical methods is essential.

Aside from extensive investigations with **L1**, we employed our approach with initial FTIR analysis and subsequent NaOH treatment prior to NMR and CE to tridentate N-based ligands, namely, **dpa**, **dien**, and two triazacyclononane derivatives. Likewise, these ligands were incapable of promoting the formation of oxalate when combined with CuI and $NaBPh_4$ under the studied conditions. For reactions with **dien**, a blank experiment in the absence of CO_2 was performed to demonstrate that the observed signal in the CE likely corresponded to I^-, thereby highlighting another valuable tool for studying CO_2 reductive coupling.

Finally, we investigated whether a structurally similar dinuclear Cu complex derived from **L4** might be active in the conversion of CO_2 into oxalate. Analogous 1,8-bis((1,4,7-triazacyclononanyl)methyl)naphthalene (**18**) was reported to serve as a valuable ligand for the detection of $C_2O_4^{2-}$ via fluorescence spectroscopy in combination with Eosin-Y due to selective binding to the derived Cu complex.[92] The ability of **L4** to coordinate two Cu centers was established by the synthesis of [Cu_2(**L4**)I_2] (**19**). However, **L4** did not facilitate the formation of oxalate when combined with CuI or CuI/$NaBPh_4$. Again, ESI-HRMS was employed to assign the CE signal with fitting migration time to I^- rather than oxalate. In addition, a reaction with $^{13}CO_2$ was conducted to further corroborate this assignment by the absence of the ^{13}C NMR signal of $C_2O_4^{2-}$.

Moreover, GC analysis of the reaction headspace for selected examples combined with ^{13}C NMR spectroscopy provided no evidence for substantial CO_2 reduction with the investigated Cu^I complexes, albeit formate traces were identified for few reactions (also under oxidative conditions in air—see Table S4, entry 4). Finally, to rule out the possibility of an oxidative process yielding μ-C_2O_4 complex **2**, we treated the in situ formed [Cu^I(**L1**)X] (X = I, BPh_4) with air or O_2. Neither of these reactions resulted in oxalate formation.

In conclusion, the results from our extensive investigations with various ligands, additives, and reaction conditions (Scheme 6) highlight the problems arising from irreproducibility of CO_2 reductive coupling by a Cu complex.[71] While we cannot entirely exclude the formation of small quantities of oxalate sufficient for crystallization of the complex of interest based on the combination of analytical methods employed by us, we cannot confirm the previously reported yields for oxalate complex **2**.

Besides *irreproducibility* and *ambiguous analysis*, *conflicting reactivity* causing the formation of oxalate without incorporation of CO_2 can be misleading and constitutes another major pitfall for investigations on the reductive dimerization of CO_2.[66,72] This is showcased by the third selected example based on Cu α-ketocarboxylate complexes. In 2014, Fujisawa and co-workers reported the unusual formation of a dinuclear oxalate complex **3** ligated by $Tp^{iPr,iPr}$ which was isolated from the reaction of

Scheme 6. Irreproducibility in the Formation of Oxalate from CO_2 or $MHCO_3$ with $[Cu^I(NNN)]^+$ Complexes Studied under Various Conditions, with Multiple Ligands and Different Additives
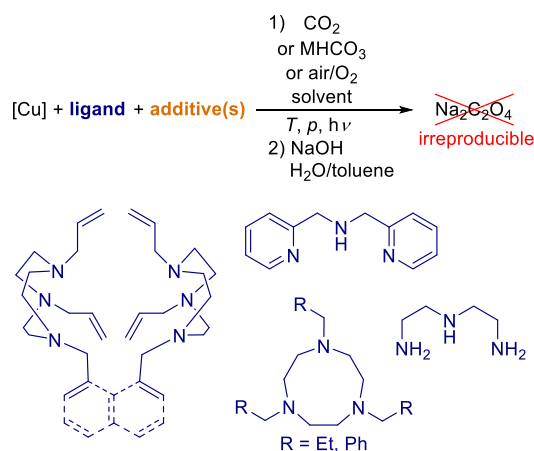
$[Cu(Tp^{iPr,iPr})(O_2CC(O)CH(CH_3)_2)]$ (**9**) with air, O_2, or CO_2/O_2.[62] The reaction was proposed to proceed via formation of a $CO_2^{\bullet-}$ intermediate resulting from decomposition of the α-ketocarboxylate in the presence of O_2. Incorporation of CO_2 into the product was evaluated with $^{13}CO_2$/O_2 causing an isotopic shift in the C–O vibration of 49 cm^{-1}. However, the demand for oxidative reaction conditions to facilitate a reduction paired with our experience on the oxidative degradation of ascorbate encouraged us to gain additional insight in the underlying reaction mechanism.

To evaluate CO_2 incorporation into oxalate, we prepared complex **9** and its ^{13}C labeled analogue **20**. It is noteworthy that our initial attempt to utilize $[(Tp^{iPr,iPr})CuBr]$ (**22**) was impeded by the formation of an undesired byproduct ($[(Hpz^{iPr})_2CuBr]$, **23**) indicating the decomposition of the $Tp^{iPr,iPr}$ ligand, an infamous property of these scorpionate ligands.[93−99]

Our initial reactions of **9** and **20** with air in CH_2Cl_2/heptane or CO_2/O_2 in toluene indeed produced oxalate. However, the obtained yields (by CE) were significantly reduced compared to the literature, and analysis by ^{13}C NMR revealed the formation of 2-hydroxy-2-methylpropanoic acid and 2-methylpropanoic acid. These products likely resulted from oxidative decarboxylation of the α-ketocarboxylate and account for the decreased $C_2O_4^{2-}$ yield. Formation of 2-hydroxy-2-methylpropanoic acid was mentioned in the original report and ascribed to dry air, highlighting the necessity of water.[62] Thus, reaction of **20** with CO_2/O_2 in toluene-d_8 with addition of D_2O was conducted and displayed enhanced selectivity for oxalate over decarboxylation products by ^{13}C NMR analysis, albeit the oxalate yield showed poor reproducibility according to CE. Interestingly, $^{13}C_3$-acetone was detected by ^{13}C NMR for this reaction prior to treatment with NaOH. This hints at a different mechanism for the formation of oxalate, namely, oxidative C2–C3 bond scission rather than the reported C1–C2 cleavage. This is further corroborated by the observation of decarboxylation products resulting from oxidative C1–C2 scission in combination with poor $C_2O_4^{2-}$ yields. Moreover, ESI-HRMS analysis was found to be a valuable tool in combination with isotopic labeling. ESI-HRMS measurements confirmed the presence of $^{13}C_2O_4^{2-}$ for reactions of **20** with air or CO_2/O_2 (in toluene-d_8/D_2O) while no mixed isotopic constitutions of oxalate were observed.

Incorporation of CO_2 via the originally proposed mechanism should partially result in mixed isotope oxalate. In contrast, should oxalate formation proceed via oxidative C2–C3 bond cleavage, one would not expect any CO_2 incorporation and, thus, no formation of $^{13}C^{12}CO_4^{2-}$. Oxidative decarboxylation of α-ketocarboxylates via C1–C2 bond cleavage is well-known for Tp complexes of Fe.[100,101] Likewise, the oxidative C2–C3 cleavage of phenylpyruvate yielding oxalate has been observed for Fe and Co complexes ligated by a trispyridylamine derivative.[100,102] Furthermore, Fe-based enzymes Dke1 (acetylacetone-cleaving enzyme) and HPPD (4-hydroxyphenylpyruvate dioxygenase) were found to convert 4-hydroxyphenylpyruvate into 4-hydroxybenzaldehyde and oxalate or 2,5-dihydroxyphenylacetic acid and CO_2, respectively.[103] These differences in reactivity are influenced by the electronic structure of the respective metal center and the ability of the α-ketocarboxylate to undergo enolization.[100,102,103]

Based on our experimental data from complexes **9** and **20**, a C2–C3 bond scission mechanism explains the formation of oxalate. These results contrast with the initially reported CO_2 incorporation based on an isotopic shift to 1607 cm^{-1} upon utilization of $^{13}CO_2$/O_2.[62] In addition, considerable quantities of decarboxylation products and low oxalate yields beg the question of how the high reported yields were obtained. Based on the selectivity enhancement upon addition of D_2O and improved $C_2O_4^{2-}$ yield after prolonged exposure to air, we envisaged that decomposition of the complexes and perhaps even $Tp^{iPr,iPr}$, as in our synthesis of $[(Tp^{iPr,iPr})CuBr]$, could occur.[93−99] The resulting Cu^{2+} might then facilitate the oxidative decomposition of the α-ketocarboxylate in analogy to its activity in the oxidation of ascorbic acid.[104,105]

Indeed, exposing a Cu^{II} precursor ($CuCl_2$ or $Cu(BF_4)_2$·$6H_2O$) and **21a** in CH_2Cl_2/MeOH/heptane to air and extracting the resulting residue with NaOH gave significantly higher oxalate yields by CE (38−82%; mononuclear yield), in accordance with the higher signal intensity in the ^{13}C NMR. Even substoichiometric quantities of $Cu(BF_4)_2$·$6H_2O$ produced 48% oxalate (by CE), while blank experiments without Cu^{2+} confirmed its role in the oxalate formation. NMR experiments with $Cu(BF_4)_2$·$6H_2O$ and **21** in CD_2Cl_2/CD_3OD or C_6D_6/CD_3OD confirmed the formation of $^{13}C_3$-acetone, which is in accordance with the proposed oxidative C2–C3 bond cleavage (Figure S131). Again, no $^{13}C^{12}CO_4^{2-}$ was detected by ESI-HRMS for reactions with **21**, highlighting the lack of CO_2 incorporation into oxalate.

For a better understanding of the proposed C2–C3 bond cleavage, the NaOH treatment was conducted under an Ar atmosphere. This resulted in a notable decrease in the oxalate yield from 48% to 17%, and unconverted α-ketocarboxylate was detected by NMR spectroscopic analysis. Hence, the basic pH facilitates the oxidative C2–C3 bond scission in the presence of Cu^{2+}. This indicates that enolization of the α-ketocarboxylate might be essential for the formation of oxalate via C2–C3 bond cleavage. To gather additional evidence for this hypothesis, further experiments were conducted with related α-ketocarboxylates. Replacement of **21a** with sodium phenylpyruvate, which would likewise allow for enolization, provided oxalate in 29% yield. In contrast, sodium pyruvate gave only 6% $C_2O_4^{2-}$, which is close to that of the blank experiment. These results further corroborate that the structure of the α-ketocarboxylate, allowing for enolization or stabilization of an intermediate radical species, is another key parameter determining the selectivity for C1–C2 vs C2–C3 bond cleavage.

Based on our experimental results, we propose the following reaction pathways for **9/20** (Scheme 7): Well-defined [Cu-

Scheme 7. Proposed Reaction Pathway for the Formation of Oxalate and Acetone via Oxidative C2−C3 Bond Cleavage[a]
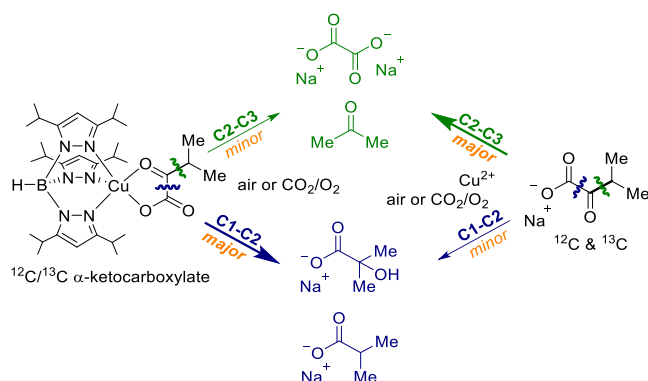
[a]Isobutyric acid and 2-hydroxyisobutyric acid were identified, presumably resulting from oxidative decarboxylation upon C1−C2 bond scission.

$(Tp^{iPr,iPr})(O_2CC(O)CH(CH_3)_2)]$ complexes facilitate primarily oxidative decarboxylation via C1−C2 bond scission. Low quantities of oxalate should be a result of C2−C3 bond cleavage by $[Cu(Tp^{iPr,iPr})]^+$ or by its decomposition products, possibly resulting from hydrolysis in the presence of H_2O. In contrast, Cu^{2+} facilitates the oxidative degradation of suitable α-ketocarboxylates into oxalate. Here, the oxidation under basic pH plays an integral part. Besides these primary reactions, the underlying oxidative degradation processes appear to be more complicated and might involve follow-up condensation reactions during NaOH treatment, as indicted by the ^{13}C NMR spectroscopic analysis (Section S7.4).

In conclusion, this example highlights that oxidative processes resulting in the formation of oxalate can readily be misinterpreted. Therefore, cautious analysis with a combination of analytical techniques as well as suitable control experiments to evaluate the incorporation of CO_2 are required to avoid this pitfall.

■ CONCLUSIONS

The use of renewable energy to produce organic matter has remained a central challenge for many decades. In this context, the reductive dimerization of carbon dioxide to oxalate can be considered as a first step. Hence, this apparently simple reaction continues to be of interest for basic science as well as more recently in the context of alternative energy technologies, highlighted by the "OCEAN" project of the European Union, which explores the conversion of CO_2 into oxalic acid and its utilization as a platform chemical.[28]

While investigating the desired CO_2 reductive dimerization, we faced significant problems and describe here the potential pitfalls based on our studies. Looking exemplarily at three previously published works, we identified irreproducibility, insufficient analysis, misleading analytical data, and conflicting reactivity as the main hurdles, which arguably hamper the development of novel and enhancement of established protocols for CO_2 reduction to oxalate.

Specifically, using [Fe(tmtaa)] and alkali metal-based reductants, we could not verify the formation of oxalate in toluene or THF previously claimed by titration with $KMnO_4$.

Yet, the importance of suitable analytical methods became apparent.

Similarly, in the presence of triazacyclonone-ligated Cu complexes, no CO_2 reductive coupling was observed. Here, various reaction parameters, additives, and tridentate ligands were used without providing $C_2O_4^{2-}$. However, the limitations of single analytical methods, namely, IR and NMR spectroscopy as well as CE, were highlighted. Fortunately, the combination of these methods and suitable control experiments offered a reliable approach to investigate CO_2 reductive coupling.

Finally, in the reaction of $[Cu(Tp^{iPr,iPr})(O_2CC(O)CH-(CH_3)_2)]$ (**9**) with air or CO_2/O_2, oxalate results from oxidative cleavage of the substrate with no evidence for CO_2 incorporation. Interestingly, formation of oxalate via oxidative decomposition of the α-ketocarboxylate was enhanced in the presence of Cu^{2+} without any additional ligand. As part of these investigations, we presented the second[66] example for a potentially misleading outcome of an isotopic labeling study with $^{13}CO_2$ within this field. Ambiguous results can arise from the formation of additional CO_2 reduction or hydration products (formate or bicarbonate), oxidative decomposition reactions resulting in the formation of carboxylic acid or carbonyl compounds, and variable solvent contamination with, e.g., DMF.

Based on all these results, we advise the following guidelines to enhance future progress in this cutting-edge field:

(a) Utilization of a combination of orthogonal analytical methods, for instance, FTIR spectroscopy combined with NMR spectroscopy and CE analysis, is indispensable. In addition, electrospray mass spectrometry, especially coupled with CE, should allow for appropriate validation of experimental results. Suitable alternatives to CE represent ion chromatography, high-performance liquid chromatography, or gas chromatography in combination with derivatization or oxidative decomposition of oxalic acid (the latter being less compatible with studying CO_2 reduction).[67,106−110] These techniques have proven reliable in the quantification of oxalate in biological samples, foods, or waters from pulp and paper processes.

(b) In general, a cautious strategy for reaction design and implementation of control reactions to exclude oxidative processes should be made. We highly encourage researchers working in this area to examine oxidative conditions or reactions under exclusion of CO_2 to validate that a reductive process accounts for the formation of $C_2O_4^{2-}$.

(c) While isotopic labeling with $^{13}CO_2$ in combination with IR spectroscopic analysis can provide valuable insight into the mechanism of oxalate formation, we would like to raise awareness of the limited significance of the assignment of a CO_2 reductive coupling mechanism based on isotopic labeling with vibrational spectroscopy as the sole analytical tool. Here, NMR spectroscopy and ESI-HRMS offer great compatibility and provide additional information to ensure the validity of the proposed mechanism and correct identification of the reaction product.

Albeit the interest in CO_2 reductive coupling seems to suffer from the variety of complications highlighted herein, we believe the area offers great potential for the fundamental understanding of the reactivity of carbon dioxide. One of the apparently simplest C−C bond formations certainly deserves more

attention, because a mechanistic understanding allowing for a general design of suitable catalysts enabling this transformation would be highly desirable in view of the need for efficient CO_2 utilization. We believe the lessons presented throughout this article will contribute to paving the way for reliable progress within this field and, hopefully, promote the development of guiding principles for the construction of $C_{\geq 2}$ compounds from CO_2.

■ ASSOCIATED CONTENT

Ⓢ Supporting Information

The Supporting Information is available free of charge at https://pubs.acs.org/doi/10.1021/jacsau.2c00005.

General information, experimental procedures, detailed experimental results, and analytical data (PDF)

■ AUTHOR INFORMATION

Corresponding Author

Matthias Beller − *Leibniz-Institut für Katalyse e.V., 18059 Rostock, Germany;* ⓞ orcid.org/0000-0001-5709-0965; Email: matthias.beller@catalysis.de

Authors

Maximilian Marx − *Leibniz-Institut für Katalyse e.V., 18059 Rostock, Germany;* ⓞ orcid.org/0000-0001-7047-1615

Holm Frauendorf − *Institut für Organische und Biomolekulare Chemie, Georg-August-Universität Göttingen, 37077 Göttingen, Germany*

Anke Spannenberg − *Leibniz-Institut für Katalyse e.V., 18059 Rostock, Germany*

Helfried Neumann − *Leibniz-Institut für Katalyse e.V., 18059 Rostock, Germany*

Complete contact information is available at:
https://pubs.acs.org/10.1021/jacsau.2c00005

Author Contributions

The manuscript was written through contributions of all authors. All authors have given approval to the final version of the manuscript.

Notes

The authors declare no competing financial interest.

Crystallographic data for **10** (2092312), **11** (2092313), **12** (2092314), **13** (2092315), **14** (2092316), **15** (2092311), **19** (2092317), **22** (2092318), and **23** (2092319) can be obtained free of charge by the joint Cambridge Crystallographic Data Centre and Fachinformationszentrum Karlsruhe via www.ccdc.cam.ac.uk/structures

■ ACKNOWLEDGMENTS

■ ABBREVIATIONS

CE, capillary electrophoresis; DCM, dichloromethane; Dipp, 2,6-di-*iso*-propylphenyl; ESI, electrospray ionization; HRMS, high resolution mass spectrometry; IR, infrared spectroscopy; NMR, nuclear magnetic resonance; tacn, 1,4,7-triazacyclononane; THF, tetrahydrofuran; H_2tmtaa, 4,11-dihydro-5,7,12,14-tetramethyldibenzo$[b,i][1,4,8,11]$-tetraazacyclotetradecine; $Tp^{iPr,iPr}$, tris(3,5-di-*iso*-propylpyrazolyl)borate; Hpz^{iPr}, 3,5-di-*iso*-propylpyrazole

■ REFERENCES

(1) Appel, A. M.; Bercaw, J. E.; Bocarsly, A. B.; Dobbek, H.; DuBois, D. L.; Dupuis, M.; Ferry, J. G.; Fujita, E.; Hille, R.; Kenis, P. J. A.; Kerfeld, C. A.; Morris, R. H.; Peden, C. H. F.; Portis, A. R.; Ragsdale, S. W.; Rauchfuss, T. B.; Reek, J. N. H.; Seefeldt, L. C.; Thauer, R. K.; Waldrop, G. L. Frontiers, Opportunities, and Challenges in Biochemical and Chemical Catalysis of CO_2 Fixation. *Chem. Rev.* **2013**, *113*, 6621−6658.

(2) Aresta, M.; Dibenedetto, A.; Angelini, A. Catalysis for the Valorization of Exhaust Carbon: From CO_2 to Chemicals, Materials, and Fuels. Technological Use of CO_2. *Chem. Rev.* **2014**, *114*, 1709−1742.

(3) Liu, Q.; Wu, L.; Fleischer, I.; Selent, D.; Franke, R.; Jackstell, R.; Beller, M. Development of a Ruthenium/Phosphite Catalyst System for Domino Hydroformylation−Reduction of Olefins with Carbon Dioxide. *Chem. Eur. J.* **2014**, *20*, 6888−6894.

(4) Wu, L.; Liu, Q.; Fleischer, I.; Jackstell, R.; Beller, M. Ruthenium-Catalysed Alkoxycarbonylation of Alkenes with Carbon Dioxide. *Nat. Commun.* **2014**, *5*, 3091.

(5) Hong, J.; Li, M.; Zhang, J.; Sun, B.; Mo, F. C-H Bond Carboxylation with Carbon Dioxide. *ChemSusChem* **2019**, *12*, 6−39.

(6) Li, H.-R.; He, L.-N. Construction of C−Cu Bond: A Useful Strategy in CO_2 Conversion. *Organometallics* **2020**, *39*, 1461−1475.

(7) Juhl, M.; Laursen, S. L. R.; Huang, Y.; Nielsen, D. U.; Daasbjerg, K.; Skrydstrup, T. Copper-Catalyzed Carboxylation of Hydroborated Disubstituted Alkenes and Terminal Alkynes with Cesium Fluoride. *ACS Catal.* **2017**, *7*, 1392−1396.

(8) Ukai, K.; Aoki, M.; Takaya, J.; Iwasawa, N. Rhodium(I)-Catalyzed Carboxylation of Aryl- and Alkenylboronic Esters with CO_2. *J. Am. Chem. Soc.* **2006**, *128*, 8706−8707.

(9) Coates, G. W.; Moore, D. R. Discrete Metal-Based Catalysts for the Copolymerization of CO_2 and Epoxides: Discovery, Reactivity, Optimization, and Mechanism. *Angew. Chem., Int. Ed.* **2004**, *43*, 6618−6639.

(10) Darensbourg, D. J. Making Plastics from Carbon Dioxide: Salen Metal Complexes as Catalysts for the Production of Polycarbonates from Epoxides and CO_2. *Chem. Rev.* **2007**, *107*, 2388−2410.

(11) Liu, Q.; Wu, L.; Jackstell, R.; Beller, M. Using Carbon Dioxide as a Building Block in Organic Synthesis. *Nat. Commun.* **2015**, *6*, 5933.

(12) Adachi, K.; Ohta, K.; Mizuno, T. Photocatalytic Reduction of Carbon Dioxide to Hydrocarbon Using Copper-Loaded Titanium Dioxide. *Sol. Energy* **1994**, *53*, 187−190.

(13) Li, N.; Wang, B.; Si, Y.; Xue, F.; Zhou, J.; Lu, Y.; Liu, M. Toward High-Value Hydrocarbon Generation by Photocatalytic Reduction of CO_2 in Water Vapor. *ACS Catal.* **2019**, *9*, 5590−5602.

(14) Xia, Y.; Xiao, K.; Cheng, B.; Yu, J.; Jiang, L.; Antonietti, M.; Cao, S. Improving Artificial Photosynthesis over Carbon Nitride by Gas−Liquid−Solid Interface Management for Full Light-Induced CO_2 Reduction to C_1 and C_2 Fuels and O_2. *ChemSusChem* **2020**, *13*, 1730−1734.

(15) Wang, L.; Wang, L.; Zhang, J.; Liu, X.; Wang, H.; Zhang, W.; Yang, Q.; Ma, J.; Dong, X.; Yoo, S. J.; Kim, J.-G.; Meng, X.; Xiao, F.-S. Selective Hydrogenation of CO_2 to Ethanol over Cobalt Catalysts. *Angew. Chem., Int. Ed.* **2018**, *57*, 6104−6108.

(16) Qian, Q.; Cui, M.; He, Z.; Wu, C.; Zhu, Q.; Zhang, Z.; Ma, J.; Yang, G.; Zhang, J.; Han, B. Highly Selective Hydrogenation of CO_2 into C_{2+} Alcohols by Homogeneous Catalysis. *Chem. Sci.* **2015**, *6*, 5685−5689.

(17) Cui, M.; Qian, Q.; He, Z.; Zhang, Z.; Ma, J.; Wu, T.; Yang, G.; Han, B. Bromide Promoted Hydrogenation of CO_2 to Higher Alcohols Using Ru−Co Homogeneous Catalyst. *Chem. Sci.* **2016**, *7*, 5200−5205.

(18) Gao, P.; Dang, S.; Li, S.; Bu, X.; Liu, Z.; Qiu, M.; Yang, C.; Wang, H.; Zhong, L.; Han, Y.; Liu, Q.; Wei, W.; Sun, Y. Direct Production of Lower Olefins from CO_2 Conversion via Bifunctional Catalysis. *ACS Catal.* **2018**, *8*, 571−578.

(19) Gao, P.; Li, S.; Bu, X.; Dang, S.; Liu, Z.; Wang, H.; Zhong, L.; Qiu, M.; Yang, C.; Cai, J.; Wei, W.; Sun, Y. Direct Conversion of CO_2 into Liquid Fuels with High Selectivity over a Bifunctional Catalyst. *Nat. Chem.* **2017**, *9*, 1019−1024.

(20) Wang, H.; Zhao, Y.; Wu, Y.; Li, R.; Zhang, H.; Yu, B.; Zhang, F.; Xiang, J.; Wang, Z.; Liu, Z. Hydrogenation of Carbon Dioxide to C_2−C_4 Hydrocarbons Catalyzed by $Pd(PtBu_3)_2$−$FeCl_2$ with Ionic Liquid as Cocatalyst. *ChemSusChem* **2019**, *12*, 4390−4394.

(21) Ni, Y.; Chen, Z.; Fu, Y.; Liu, Y.; Zhu, W.; Liu, Z. Selective Conversion of CO_2 and H_2 into Aromatics. *Nat. Commun.* **2018**, *9*, 3457.

(22) Wang, W.-H.; Himeda, Y.; Muckerman, J. T.; Manbeck, G. F.; Fujita, E. CO_2 Hydrogenation to Formate and Methanol as an Alternative to Photo- and Electrochemical CO_2 Reduction. *Chem. Rev.* **2015**, *115*, 12936−12973.

(23) Yamazaki, Y.; Takeda, H.; Ishitani, O. Photocatalytic Reduction of CO_2 Using Metal Complexes. *J. Photochem. Photobiol. C* **2015**, *25*, 106−137.

(24) Takeda, H.; Cometto, C.; Ishitani, O.; Robert, M. Electrons, Photons, Protons and Earth-Abundant Metal Complexes for Molecular Catalysis of CO_2 Reduction. *ACS Catal.* **2017**, *7*, 70−88.

(25) Francke, R.; Schille, B.; Roemelt, M. Homogeneously Catalyzed Electroreduction of Carbon Dioxide—Methods, Mechanisms, and Catalysts. *Chem. Rev.* **2018**, *118*, 4631−4701.

(26) Windle, C. D.; Perutz, R. N. Advances in Molecular Photocatalytic and Electrocatalytic CO_2 Reduction. *Coord. Chem. Rev.* **2012**, *256*, 2562−2570.

(27) Morris, A. J.; Meyer, G. J.; Fujita, E. Molecular Approaches to the Photocatalytic Reduction of Carbon Dioxide for Solar Fuels. *Acc. Chem. Res.* **2009**, *42*, 1983−1994.

(28) Schuler, E.; Demetriou, M.; Shiju, N. R.; Gruter, G.-J. M. Towards Sustainable Oxalic Acid from CO_2 and Biomass. *ChemSusChem* **2021**, *14*, 3636−3664.

(29) Murcia Valderrama, M. A.; van Putten, R.-J.; Gruter, G.-J. M. The Potential of Oxalic − and Glycolic Acid Based Polyesters (Review). Towards CO_2 as a Feedstock (Carbon Capture and Utilization − CCU). *Eur. Polym. J.* **2019**, *119*, 445−468.

(30) Abraham, F.; Arab-Chapelet, B.; Rivenet, M.; Tamain, C.; Grandjean, S. Actinide Oxalates, Solid State Structures and Applications. *Coord. Chem. Rev.* **2014**, *266−267*, 28−68.

(31) Tyssee, D. A.; Wagenknecht, J. H.; Baizer, M. M.; Chruma, J. L. Some Cathodic Organic Syntheses Involving Carbon Dioxide. *Tetrahedron Lett.* **1972**, *13*, 4809−4812.

(32) Amatore, C.; Saveant, J. M. Mechanism and Kinetic Characteristics of the Electrochemical Reduction of Carbon Dioxide in Media of Low Proton Availability. *J. Am. Chem. Soc.* **1981**, *103*, 5021−5023.

(33) Gennaro, A.; Isse, A. A.; Savéant, J.-M.; Severin, M.-G.; Vianello, E. Homogeneous Electron Transfer Catalysis of the Electrochemical Reduction of Carbon Dioxide. Do Aromatic Anion Radicals React in an Outer-Sphere Manner? *J. Am. Chem. Soc.* **1996**, *118*, 7190−7196.

(34) Gennaro, A.; Isse, A. A.; Severin, M.-G.; Vianello, E.; Bhugun, I.; Saveant, J.-M. Mechanism of the Electrochemical Reduction of Carbon Dioxide at Inert Electrodes in Media of Low Proton Availability. *J. Chem. Soc., Faraday Trans.* **1996**, *92*, 3963−3968.

(35) Kushi, Y.; Nagao, H.; Nishioka, T.; Isobe, K.; Tanaka, K. Oxalate Formation in Electrochemical CO_2 Reduction Catalyzed by Rhodium-Sulfur Cluster. *Chem. Lett.* **1994**, *23*, 2175−2178.

(36) Tanaka, K.; Kushi, Y.; Tsuge, K.; Toyohara, K.; Nishioka, T.; Isobe, K. Catalytic Generation of Oxalate through a Coupling Reaction of Two CO_2 Molecules Activated on $[(Ir(\eta^5-C_5Me_5))_2(Ir(\eta^4-C_5Me_5)-CH_2CN)(\mu_3-S)_2]$. *Inorg. Chem.* **1998**, *37*, 120−126.

(37) Ali, M. M.; Sato, H.; Mizukawa, T.; Tsuge, K.; Haga, M.; Tanaka, K. Selective Formation of HCO_2^- and $C_2O_4^{2-}$ in Electrochemical Reduction of CO_2 Catalyzed by Mono- and Di-Nuclear Ruthenium Complexes. *Chem. Commun.* **1998**, 249−250.

(38) Rudolph, M.; Dautz, S.; Jäger, E.-G. Macrocyclic $[N_4^{2-}]$ Coordinated Nickel Complexes as Catalysts for the Formation of Oxalate by Electrochemical Reduction of Carbon Dioxide. *J. Am. Chem. Soc.* **2000**, *122*, 10821−10830.

(39) Angamuthu, R.; Byers, P.; Lutz, M.; Spek, A. L.; Bouwman, E. Electrocatalytic CO_2 Conversion to Oxalate by a Copper Complex. *Science* **2010**, *327*, 313−315.

(40) Udugala-Ganehenege, M. Y.; Dissanayake, N. M.; Liu, Y.; Bond, A. M.; Zhang, J. Electrochemistry of Nickel(II) and Copper(II) N,N'-Ethylenebis(acetylacetoniminato) Complexes and Their Electrocatalytic Activity for Reduction of Carbon Dioxide and Carboxylic Acid Protons. *Transit. Metal Chem.* **2014**, *39*, 819−830.

(41) Becker, J. Y.; Vainas, B.; Eger, R.; Kaufman, L. Electrocatalytic Reduction of CO_2 to Oxalate by Ag and Pd Porphyrins. *J. Chem. Soc., Chem. Commun.* **1985**, 1471−1472.

(42) Fröhlich, H.-O.; Schreer, H. Einschub Und Reduktive Kopplung von CO_2; Zur Bildung von $Cp_2Ti^{III}C_2O_4Ti^{III}Cp_2$ Und $Cp_2Ti^{IV}(^-O_2C-(CH_2)_3NRCH_2CH_2NR(CH_2)_3CO_2^-)$ (R = i-C_4H_9). *Z. Chem.* **1983**, *23*, 348−349.

(43) Lalrempuia, R.; Stasch, A.; Jones, C. The Reductive Disproportionation of CO_2 Using a Magnesium(I) Complex: Analogies with Low Valent f-Block Chemistry. *Chem. Sci.* **2013**, *4*, 4383−4388.

(44) Paparo, A.; Silvia, J. S.; Kefalidis, C. E.; Spaniol, T. P.; Maron, L.; Okuda, J.; Cummins, C. C. A Dimetalloxycarbene Bonding Mode and Reductive Coupling Mechanism for Oxalate Formation from CO_2. *Angew. Chem., Int. Ed.* **2015**, *54*, 9115−9119.

(45) Woen, D. H.; Chen, G. P.; Ziller, J. W.; Boyle, T. J.; Furche, F.; Evans, W. J. Solution Synthesis, Structure, and CO_2 Reduction Reactivity of a Scandium(II) Complex, $\{Sc[N(SiMe_3)_2]_3\}^-$. *Angew. Chem., Int. Ed.* **2017**, *56*, 2050−2053.

(46) Evans, W. J.; Seibel, C. A.; Ziller, J. W. Organosamarium-Mediated Transformations of CO_2 and COS: Monoinsertion and Disproportionation Reactions and the Reductive Coupling of CO_2 to $[O_2CCO_2]^{2-}$. *Inorg. Chem.* **1998**, *37*, 770−776.

(47) Evans, W. J.; Perotti, J. M.; Brady, J. C.; Ziller, J. W. Tethered Olefin Studies of Alkene versus Tetraphenylborate Coordination and Lanthanide Olefin Interactions in Metallocenes. *J. Am. Chem. Soc.* **2003**, *125*, 5204−5212.

(48) Willauer, A. R.; Toniolo, D.; Fadaei-Tirani, F.; Yang, Y.; Laurent, M.; Mazzanti, M. Carbon Dioxide Reduction by Dinuclear Yb(II) and Sm(II) Complexes Supported by Siloxide Ligands. *Dalton Trans.* **2019**, *48*, 6100−6110.

(49) Castro, L.; Mills, D. P.; Jones, C.; Maron, L. Activation of Heteroallenes CO_xS_{2-x} (x = 0−2): Experimental and Theoretical Evidence of the Synthetic Versatility of a Bulky Guanidinato Sm^{II} Complex. *Eur. J. Inorg. Chem.* **2016**, *2016*, 792−796.

(50) Andrez, J.; Pécaut, J.; Bayle, P.-A.; Mazzanti, M. Tuning Lanthanide Reactivity Towards Small Molecules with Electron-Rich Siloxide Ligands. *Angew. Chem., Int. Ed.* **2014**, *53*, 10448−10452.

(51) Wong, W.-K.; Zhang, L.-L.; Xue, F.; Mak, T. C. W. Synthesis and X-Ray Crystal Structure of an Unexpected Neutral Oxalate-Bridged Ytterbium(III) Porphyrinate Dimer. *J. Chem. Soc., Dalton Trans.* **2000**, 2245−2246.

(52) Evans, W. J.; Lorenz, S. E.; Ziller, J. W. Investigating Metal Size Effects in the $Ln_2(\mu-\eta^2:\eta^2-N_2)$ Reduction System: Reductive Reactivity with Complexes of the Largest and Smallest Trivalent Lanthanide Ions, La^{3+} and Lu^{3+}. *Inorg. Chem.* **2009**, *48*, 2001−2009.

(53) Tsoureas, N.; Castro, L.; Kilpatrick, A. F. R.; Cloke, F. G. N.; Maron, L. Controlling Selectivity in the Reductive Activation of CO_2 by Mixed Sandwich Uranium(III) Complexes. *Chem. Sci.* **2014**, *5*, 3777−3788.

(54) Inman, C. J.; Frey, A. S. P.; Kilpatrick, A. F. R.; Cloke, F. G. N.; Roe, S. M. Carbon Dioxide Activation by a Uranium(III) Complex Derived from a Chelating Bis(aryloxide) Ligand. *Organometallics* **2017**, *36*, 4539−4545.

(55) Schmidt, A.-C.; Heinemann, F. W.; Kefalidis, C. E.; Maron, L.; Roesky, P. W.; Meyer, K. Activation of SO_2 and CO_2 by Trivalent Uranium Leading to Sulfite/Dithionite and Carbonate/Oxalate Complexes. *Chem. Eur. J.* **2014**, *20*, 13501−13506.

(56) Formanuik, A.; Ortu, F.; Inman, C. J.; Kerridge, A.; Castro, L.; Maron, L.; Mills, D. P. Concomitant Carboxylate and Oxalate Formation From the Activation of CO_2 by a Thorium(III) Complex. *Chem. Eur. J.* **2016**, *22*, 17976−17979.

(57) Aresta, M.; Gobetto, R.; Quaranta, E.; Tommasi, I. A Bonding-Reactivity Relationship for $Ni(PCy_3)_2(CO_2)$: A Comparative Solid-State-Solution Nuclear Magnetic Resonance Study (^{31}P, ^{13}C) as a Diagnostic Tool to Determine the Mode of Bonding of CO_2 to a Metal Center. *Inorg. Chem.* **1992**, *31*, 4286−4290.

(58) Horn, B.; Limberg, C.; Herwig, C.; Braun, B. Nickel(I)-Mediated Transformations of Carbon Dioxide in Closed Synthetic Cycles: Reductive Cleavage and Coupling of CO_2 Generating Ni^ICO, $Ni^{II}CO_3$ and $Ni^{II}C_2O_4Ni^{II}$ Entities. *Chem. Commun.* **2013**, *49*, 10923−10925.

(59) Lu, C. C.; Saouma, C. T.; Day, M. W.; Peters, J. C. Fe(I)-Mediated Reductive Cleavage and Coupling of CO_2: An $Fe^{II}(\mu$-O,μ-CO)Fe^{II} Core. *J. Am. Chem. Soc.* **2007**, *129*, 4−5.

(60) Saouma, C. T.; Lu, C. C.; Day, M. W.; Peters, J. C. CO_2 Reduction by Fe(I): Solvent Control of C-O Cleavage versus C-C Coupling. *Chem. Sci.* **2013**, *4*, 4042−4051.

(61) Farrugia, L. J.; Lopinski, S.; Lovatt, P. A.; Peacock, R. D. Fixing Carbon Dioxide with Copper: Crystal Structure of $[LCu(\mu$-$C_2O_4)$-CuL][Ph_4B]_2$ (L = *N,N′,N″*-triallyl-1,4,7-triazacyclononane). *Inorg. Chem.* **2001**, *40*, 558−559.

(62) Takisawa, H.; Morishima, Y.; Soma, S.; Szilagyi, R. K.; Fujisawa, K. Conversion of Carbon Dioxide to Oxalate by α-Ketocarboxylatocopper(II) Complexes. *Inorg. Chem.* **2014**, *53*, 8191−8193.

(63) Klose, A.; Hesschenbrouck, J.; Solari, E.; Latronico, M.; Floriani, C.; Re, N.; Chiesi-Villa, A.; Rizzoli, C. The Metal−Carbon Multiple Bond in Iron(I)− and Iron(II)−Dibenzotetramethyltetra-[14]-azaannulene: Carbene, Carbonyl, and Isocyanide Derivatives. *J. Organomet. Chem.* **1999**, *591*, 45−62.

(64) Tseng, Y.-T.; Ching, W.-M.; Liaw, W.-F.; Lu, T.-T. Dinitrosyl Iron Complex $[K$-18-crown-6-ether]$[(NO)_2Fe(^{Me}PyrCO_2)]$: Intermediate for Capture and Reduction of Carbon Dioxide. *Angew. Chem., Int. Ed.* **2020**, *59*, 11819−11823.

(65) Cook, B. J.; Di Francesco, G. N.; Abboud, K. A.; Murray, L. J. Countercations and Solvent Influence CO_2 Reduction to Oxalate by Chalcogen-Bridged Tricopper Cyclophanates. *J. Am. Chem. Soc.* **2018**, *140*, 5696−5700.

(66) Khamespanah, F.; Marx, M.; Crochet, D. B.; Pokharel, U. R.; Fronczek, F. R.; Maverick, A. W.; Beller, M. Oxalate Production via Oxidation of Ascorbate Rather than Reduction of Carbon Dioxide. *Nat. Commun.* **2021**, *12*, 1997.

(67) Häärä, M.; Sundberg, A.; Willför, S. Calcium Oxalate - a Source of "Hickey" Problems - A Literature Review on Oxalate Formation, Analysis and Scale Control. *Nord. Pulp. Paper Res. J.* **2011**, *26*, 263−282.

(68) Nelson, B. C.; Rockwell, G. F.; Campfield, T.; O'Grady, P.; Hernandez, R. M.; Wise, S. A. Capillary Electrophoretic Determination of Oxalate in Amniotic Fluid. *Anal. Chim. Acta* **2000**, *410*, 1−10.

(69) Chai, W.; Liebman, M. Oxalate Content of Legumes, Nuts, and Grain-Based Flours. *J. Food Compost. Anal.* **2005**, *18*, 723−729.

(70) Sirén, H.; Kokkonen, R.; Hiissa, T.; Särme, T.; Rimpinen, O.; Laitinen, R. Determination of Soluble Anions and Cations from Waters of Pulp and Paper Mills with On-Line Coupled Capillary Electrophoresis. *J. Chromatogr. A* **2000**, *895*, 189−196.

(71) Thomas, A. M.; Lin, B.-L.; Wasinger, E. C.; Stack, T. D. P. Ligand Noninnocence of Thiolate/Disulfide in Dinuclear Copper Complexes: Solvent-Dependent Redox Isomerization and Proton-Coupled Electron Transfer. *J. Am. Chem. Soc.* **2013**, *135*, 18912−18919.

(72) Knope, K. E.; Kimura, H.; Yasaka, Y.; Nakahara, M.; Andrews, M. B.; Cahill, C. L. Investigation of in Situ Oxalate Formation from 2,3-Pyrazinedicarboxylate under Hydrothermal Conditions Using Nuclear Magnetic Resonance Spectroscopy. *Inorg. Chem.* **2012**, *51*, 3883−3890.

(73) Connelly, N. G.; Geiger, W. E. Chemical Redox Agents for Organometallic Chemistry. *Chem. Rev.* **1996**, *96*, 877−910.

(74) Drew, M. G. B.; Cairns, C.; McFall, S. G.; Nelson, S. M. The Synthesis, Properties, and the Crystal and Molecular Structures of Five-Co-Ordinate Copper(I) and Silver(I) Complexes of a Quinquedentate Macrocyclic Ligand Having an 'N₃S₂' Donor Set. *J. Chem. Soc., Dalton Trans.* **1980**, 2020−2027.

(75) Crystals of $[Cu(\mathbf{L1})I]$ were obtained from a THF solution of in situ formed $[Cu(\mathbf{L1})I]$ starting from CuI, $\mathbf{L1}$, and NaBPh_4. This indicates incomplete iodo exchange with NaBPh_4. $[Cu(\mathbf{L1})I]$ was independently synthesized (experimental procedure and analytical data can be found in the Supporting Information).

(76) Farrugia, L. J.; Lovatt, P. A.; Peacock, R. D. Macrocycles with a Single Pendant Arm: Synthesis of *N*-R-(1,4,7-triazacyclononane) [L, R = 4-but-1-ene; L′, R = 3-prop-1-ene]: Synthesis of the Cu^I Complex $[CuL]I$ and Synthesis and Crystal Structure of the Cu^{II} Complex $[CuL_2][BPh_4]_2$ and the μ-Hydroxy Bridged Cu^{II} Dimer $[LCu(\mu$-$OH)_2CuL][BPh_4]_2$. *Inorg. Chim. Acta* **1996**, *246*, 343−348.

(77) Farrugia, L. J.; Lovatt, P. A.; Peacock, R. D. Synthesis of a series of novel binucleating ligands based on 1,4,7-triazacyclononane and *o*-, *m*- and *p*-xylene: crystal structure of the μ-hydroxy-bridged dicopper(II) complex $[Cu_2L^m(OH)_2][BPh_4]_2$ $[L^m = \alpha,\alpha'$-bis(*N*-1,4,7-triazacyclononane)-*m*-xylene]. *J. Chem. Soc., Dalton Trans.* **1997**, 911−912.

(78) Agilent Technologies. *User Manual: Organic Acids Analysis Kit, PN 5063-6510* https://www.agilent.com/cs/library/usermanuals/public/5968-9047E_print.pdf.pdf (accessed 2021-06-25).

(79) Zhang, X.; Hsieh, W.-Y.; Margulis, T. N.; Zompa, L. J. Binuclear Copper(II) Complexes of Bis(1,4,7-triazacyclononane) Ligands Containing Tri- and Tetramethylene Bridging Groups. An Equilibrium and Structural Study. *Inorg. Chem.* **1995**, *34*, 2883−2888.

(80) Young, M. J.; Chin, J. Dinuclear Copper(II) Complex That Hydrolyzes RNA. *J. Am. Chem. Soc.* **1995**, *117*, 10577−10578.

(81) McBride, R. S. The Standardization of Potassium Permanganate Solution by Sodium Oxalate. *J. Am. Chem. Soc.* **1912**, *34*, 393−416.

(82) Knocke, W. R.; van Benschoten, J. E.; Kearney, M. J.; Soborski, A. W.; Reckhow, D. A. Kinetics of Manganese and Iron Oxidation by Potassium Permanganate and Chlorine Dioxide. *J. Am. Water Works Assoc.* **1991**, *83*, 80−87.

(83) Singh, N.; Lee, D. G. Permanganate: A Green and Versatile Industrial Oxidant. *Org. Process Res. Dev.* **2001**, *5*, 599−603.

(84) Mahapatra, S.; Halfen, J. A.; Wilkinson, E. C.; Pan, G.; Cramer, C. J.; Que, L.; Tolman, W. B. A New Intermediate in Copper Dioxygen Chemistry: Breaking the O-O Bond To Form a $\{Cu_2(\mu$-$O)_2\}^{2+}$ Core. *J. Am. Chem. Soc.* **1995**, *117*, 8865−8866.

(85) Mahapatra, S.; Halfen, J. A.; Wilkinson, E. C.; Pan, G.; Wang, X.; Young, V. G.; Cramer, C. J.; Que, L.; Tolman, W. B. Structural, Spectroscopic, and Theoretical Characterization of Bis(μ-oxo)dicopper Complexes, Novel Intermediates in Copper-Mediated Dioxygen Activation. *J. Am. Chem. Soc.* **1996**, *118*, 11555−11574.

(86) Mahapatra, S.; Young, V. G., Jr.; Kaderli, S.; Zuberbühler, A. D.; Tolman, W. B. Tuning the Structure and Reactivity of the $[Cu_2(\mu$-$O)_2]^{2+}$ Core: Characterization of a New Bis(μ-oxo)dicopper Complex Stabilized by a Sterically Hindered Dinucleating Bis(triazacylononane) Ligand. *Angew. Chem., Int. Ed.* **1997**, *36*, 130−133.

(87) Dalle, K. E.; Gruene, T.; Dechert, S.; Demeshko, S.; Meyer, F. Weakly Coupled Biologically Relevant $Cu^{II}_2(\mu$-η^1:η^1-$O_2)$ *cis*-Peroxo Adduct that Binds Side-On to Additional Metal Ions. *J. Am. Chem. Soc.* **2014**, *136*, 7428−7434.

(88) Haidar, R.; Ipek, M.; DasGupta, B.; Yousaf, M.; Zompa, L. J. Copper(II) Complexes of Bis(1,4,7-triazacyclononane) Ligands with Polymethylene Bridging Groups: An Equilibrium and Structural Study. *Inorg. Chem.* **1997**, *36*, 3125−3132.

(89) Halfen, J. A.; Young, V. G.; Tolman, W. B. Dioxygen Activation by a Copper(I) Complex of a New Tetradentate Tripodal Ligand:

Mechanistic Insights into Peroxodicopper Core Reactivity. *J. Am. Chem. Soc.* **1996**, *118*, 10920−10921.

(90) Houser, R. P.; Halfen, J. A.; Young, V. G.; Blackburn, N. J.; Tolman, W. B. Structural Characterization of the First Example of a Bis(μ-thiolato)dicopper(II) Complex. Relevance to Proposals for the Electron Transfer Sites in Cytochrome *c* Oxidase and Nitrous Oxide Reductase. *J. Am. Chem. Soc.* **1995**, *117*, 10745−10746.

(91) Houser, R. P.; Young, V. G.; Tolman, W. B. A Thiolate-Bridged, Fully Delocalized Mixed-Valence Dicopper(I, II) Complex That Models the Cu$_A$ Biological Electron-Transfer Site. *J. Am. Chem. Soc.* **1996**, *118*, 2101−2102.

(92) Tang, L.; Park, J.; Kim, H.-J.; Kim, Y.; Kim, S. J.; Chin, J.; Kim, K. M. Tight Binding and Fluorescent Sensing of Oxalate in Water. *J. Am. Chem. Soc.* **2008**, *130*, 12606−12607.

(93) Cano, M.; Heras, J. V.; Santamaria, E.; Pinilla, E.; Monge, A.; Jones, C. J.; McCleverty, J. A. Trispyrazolylborate Degradation and the Crystal Structure of [Mo(NO)(CO)$_2${HB(OPr^i)(3-Pr^i-5-MeC$_3$HN$_2$)$_2$}]. *Polyhedron* **1993**, *12*, 1711−1714.

(94) Bellachioma, G.; Cardaci, G.; Gramlich, V.; Macchioni, A.; Pieroni, F.; Venanzi, L. M. Synthesis and Characterisation of Bis- and Tris-(pyrazol-1-yl)borate Acetyl Complexes of Fe^{II} and Ru^{II} and Isolation of an Intermediate of B−N Bond Hydrolysis. *J. Chem. Soc., Dalton Trans.* **1998**, 947−952.

(95) Lee, C.-L.; Wu, Y.-Y.; Wu, C.-P.; Chen, J.-D.; Keng, T.-C.; Wang, J.-C. Synthesis and Structural Characterization of Face-Sharing Bioctahedral Complexes Containing Poly(pyrazolyl)borate Ligands: [HB(Me$_2$Pz)$_3$BH][X$_3$Mo(μ-X)$_2$(μ-H)MoTp*] (X = Cl or Br; Tp*=HB(Me$_2$Pz)$_3$; Pz = pyrazolyl). *Inorg. Chim. Acta* **1999**, *292*, 182−188.

(96) Chia, L. M. L.; Radojevic, S.; Scowen, I. J.; McPartlin, M.; Halcrow, M. A. Steric Control of the Reactivity of Moderately Hindered Tris(pyrazolyl)borates with Copper(II) Salts. *J. Chem. Soc., Dalton Trans.* **2000**, 133−140.

(97) Carmona, E.; Cingolani, A.; Marchetti, F.; Pettinari, C.; Pettinari, R.; Skelton, B. W.; White, A. H. Synthesis and Structural Characterization of Mixed-Sandwich Complexes of Rhodium(III) and Iridium-(III) with Cyclopentadienyl and Hydrotris(pyrazolyl)borate Ligands. *Organometallics* **2003**, *22*, 2820−2826.

(98) Morawitz, T.; Zhang, F.; Bolte, M.; Bats, J. W.; Lerner, H.-W.; Wagner, M. Di- and Tritopic Poly(pyrazol-1-yl)borate Ligands: Synthesis, Characterization, and Reactivity toward [Mn(CO)$_5$Br]. *Organometallics* **2008**, *27*, 5067−5074.

(99) Harding, D. J.; Harding, P.; Daengngern, R.; Yimklan, S.; Adams, H. Synthesis and Characterization of Redox-Active Tris(pyrazolyl)-borate Cobalt Complexes. *Dalton Trans.* **2009**, 1314−1320.

(100) Paine, T. K.; Zheng, H.; Que, L. Iron Coordination Chemistry of Phenylpyruvate: An Unexpected κ^3-Bridging Mode That Leads to Oxidative Cleavage of the C2-C3 Bond. *Inorg. Chem.* **2005**, *44*, 474−476.

(101) Mukherjee, A.; Cranswick, M. A.; Chakrabarti, M.; Paine, T. K.; Fujisawa, K.; Münck, E.; Que, L. Oxygen Activation at Mononuclear Nonheme Iron Centers: A Superoxo Perspective. *Inorg. Chem.* **2010**, *49*, 3618−3628.

(102) Chakraborty, B.; Halder, P.; Banerjee, P. R.; Paine, T. K. Oxidative C−C Bond Cleavage of α-Keto Acids by Cobalt(II) Complexes of Nitrogen Donor Ligands. *Eur. J. Inorg. Chem.* **2012**, *2012*, 5843−5853.

(103) Diebold, A. R.; Straganz, G. D.; Solomon, E. I. Spectroscopic and Computational Studies of α-Keto Acid Binding to Dke1: Understanding the Role of the Facial Triad and the Reactivity of β-Diketones. *J. Am. Chem. Soc.* **2011**, *133*, 15979−15991.

(104) Davies, M. B. Reactions of L-Ascorbic Acid with Transition Metal Complexes. *Polyhedron* **1992**, *11*, 285−321.

(105) Shen, J.; Griffiths, P. T.; Campbell, S. J.; Utinger, B.; Kalberer, M.; Paulson, S. E. Ascorbate Oxidation by Iron, Copper and Reactive Oxygen Species: Review, Model Development, and Derivation of Key Rate Constants. *Sci. Rep.* **2021**, *11*, 7417.

(106) Peldszus, S.; Huck, P. M.; Andrews, S. A. Quantitative Determination of Oxalate and Other Organic Acids in Drinking Water at Low μg/l Concentrations. *J. Chromatogr. A* **1998**, *793*, 198−203.

(107) Li, H.; Liu, Y.; Zhang, Q.; Zhan, H. Determination of the Oxalate Content in Food by Headspace Gas Chromatography. *Anal. Methods* **2014**, *6*, 3720−3723.

(108) Li, H.; Chai, X.-S.; DeMartini, N.; Zhan, H.; Fu, S. Determination of Oxalate in Black Liquor by Headspace Gas Chromatography. *J. Chromatogr. A* **2008**, *1192*, 208−211.

(109) Judprasong, K.; Charoenkiatkul, S.; Sungpuag, P.; Vasanachitt, K.; Nakjamanong, Y. Total and Soluble Oxalate Contents in Thai Vegetables, Cereal Grains and Legume Seeds and Their Changes after Cooking. *J. Food Compost. Anal.* **2006**, *19*, 340−347.

(110) Clausen, C. A.; Kenealy, W.; Lebow, P. K. Oxalate Analysis Methodology for Decayed Wood. *Int. Biodeter. Biodegr.* **2008**, *62*, 372−375.